

Imaging of metastatic melanoma

Poster No.: C-1191
Congress: ECR 2016
Type: Educational Exhibit
Authors: B. Peters¹, F. M. H. M. Vanhoenacker¹, J. Waegemans², C. De Fré¹, A. Snoeckx³, P. M. Parizel⁴; ¹Antwerp/BE, ²Duffel/BE, ³Edegem/BE, ⁴Antwerp (Edegem)/BE
Keywords: Oncology, CT, PET-CT, MR, Staging, Metastases
DOI: 10.1594/ecr2016/C-1191

Any information contained in this pdf file is automatically generated from digital material submitted to EPOS by third parties in the form of scientific presentations. References to any names, marks, products, or services of third parties or hypertext links to third-party sites or information are provided solely as a convenience to you and do not in any way constitute or imply ECR's endorsement, sponsorship or recommendation of the third party, information, product or service. ECR is not responsible for the content of these pages and does not make any representations regarding the content or accuracy of material in this file.

As per copyright regulations, any unauthorised use of the material or parts thereof as well as commercial reproduction or multiple distribution by any traditional or electronically based reproduction/publication method is strictly prohibited.

You agree to defend, indemnify, and hold ECR harmless from and against any and all claims, damages, costs, and expenses, including attorneys' fees, arising from or related to your use of these pages.

Please note: Links to movies, ppt slideshows and any other multimedia files are not available in the pdf version of presentations.

www.myESR.org

Learning objectives

1. To demonstrate the merit of each imaging technique in the evaluation of metastatic spread of melanoma.
2. To discuss the potential patterns and location of distant dissemination of melanoma.

Background

Primary melanoma

Definition:

-Aggressive tumor originating from melanocytes.

Epidemiology:

-2,2-19,2/100 000 in Europe

-1,5/100 000 mortality rate

Risk factors:

- White race
- Sun sensitivity
- Severe sunburns
- Many moles
- Freckles
- Family history of skin cancer

Primary Melanoma workout:

-Breslow and Clark for staging primary lesion

-TNM classification:

- Breslow thickness

- Clark level
- Locoregional metastasis
- Distant metastasis
- Serum LDH is an independent prognostic factor aside from the location of metastasis

-Poor prognosis for advanced disease

Disease staging is performed using the TNM classification on a clinical or pathological base ([Table 1](#) on page 4).

Imaging plays a pivotal role in the staging, follow-up and monitoring of treatment response of malignant melanoma.

The purpose of this poster is to evaluate the potential patterns and location of distant dissemination and the merit of each imaging technique in the evaluation of metastatic spread.

Metastatic melanoma

Definition:

Metastatic melanoma is tumor spread beyond the primary lesion. Tumor dissemination occurs through lymphatic or hematogenous spread [Fig. 1](#) on page 4. Metastasis is subdivided in locoregional metastasis [Fig. 2](#) on page 5 or distant metastasis. Locoregional metastasis mainly occurs through lymphatic spread.

Locoregional metastasis:

- Local recurrences
- Satellite metastasis [Fig. 3](#) on page 6
- In-transit metastasis [Fig. 4](#) on page 7
- Nodal basin

Distant metastasis are classified in 3 groups, according to the site of metastasis and serum LDH:

- M1a: Metastasis to distant skin, subcutaneous tissue or distant lymph nodes with a normal serum LDH
- M1b: Metastasis to the lung with a normal serum LDH
- M1c: Metastasis to any other visceral organ with a normal serum LDH or with any metastasis with an elevated serum LDH

Images for this section:

Clinical Staging				Pathologic staging			
				T	N	M	
	0 Tis	N0	M0		0 Tis	N0	M0
IA	T1a	N0	M0	IA	T1a	N0	M0
IB	T1b	N0	M0	IB	T1b	N0	M0
	T2a	N0	M0		T2a	N0	M0
IIA	T2b	N0	M0	IIA	T2b	N0	M0
	T3a	N0	M0		T3a	N0	M0
IIB	T3b	N0	M0	IIB	T3b	N0	M0
	T4a	N0	M0		T4a	N0	M0
IIC	T4b	N0	M0	IIC	T4b	N0	M0
III	Any T	N>N0	M0	IIIA	T1-4a	N1a	M0
					T1-4a	N2a	M0
				IIIB	T1-4b	N1a	M0
					T1-4b	N2a	M0
					T1-4a	N1b	M0
					T1-4a	N2b	M0
					T1-4a	N2c	M0
				IIIC	T1-4b	N1b	M0
					T1-4b	N2b	M0
					T1-4b	N2c	M0
					Any T	N3	M0
IV	Any T	Any N	M1	IV	Any T	Any N	M1

Table 1: Table of the clinical and pathologic TNM classification. Further discussion is beyond the scope of this poster. Further down this poster, we will point out when imaging for metastatic melanoma is indicated in asymptomatic patients.

© Department of Radiology, University Hospital Antwerp - Antwerp/BE

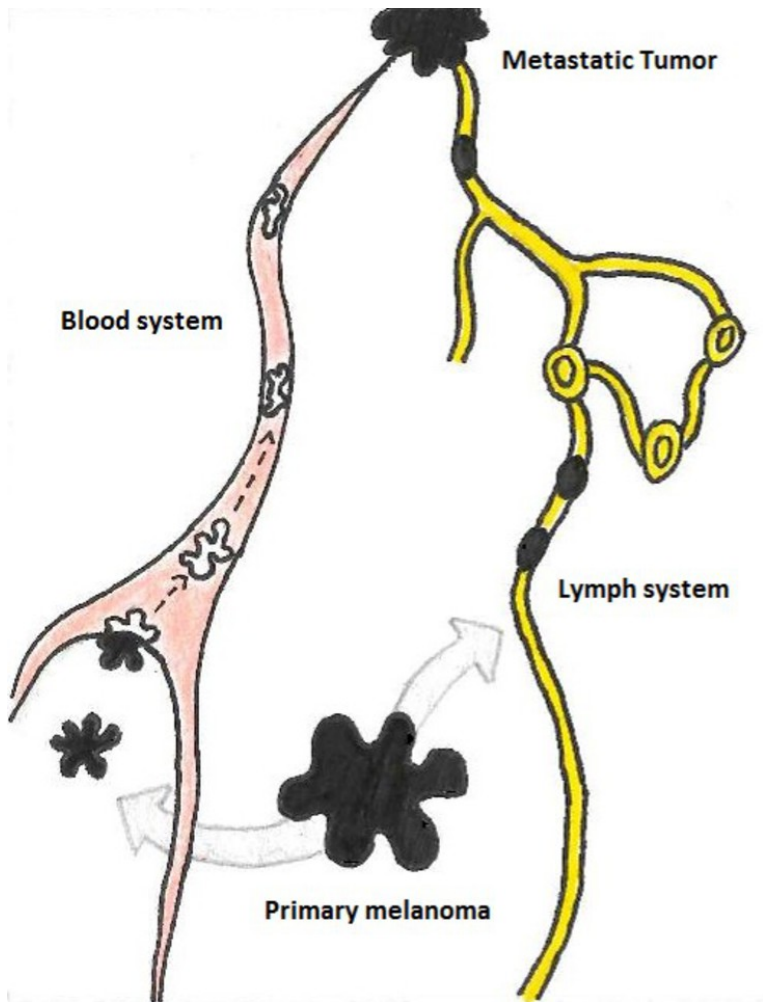


Fig. 1: Schematic drawing of hematogenous and lymphatic dissemination.

© Department of Radiology, University Hospital Antwerp - Antwerp/BE

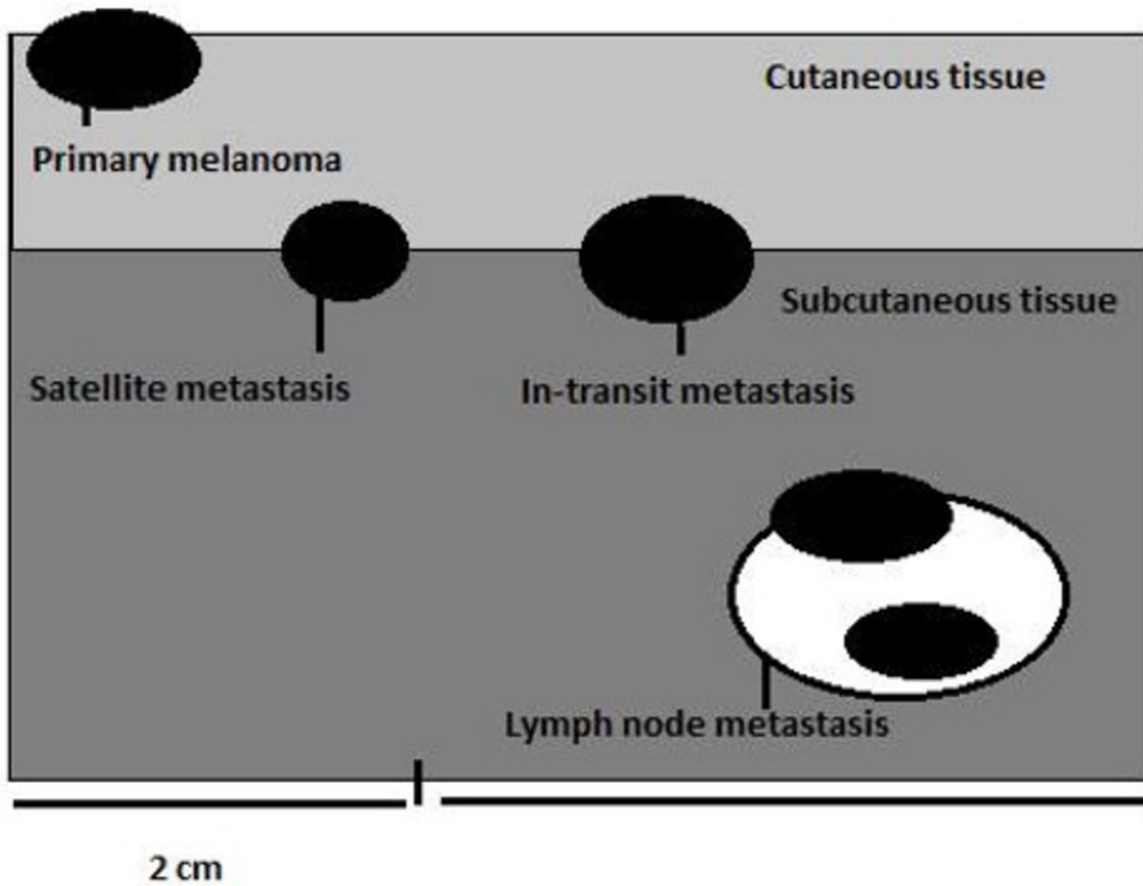


Fig. 2: Schematic drawing of locoregional metastasis.

© Department of Radiology, University Hospital Antwerp - Antwerp/BE

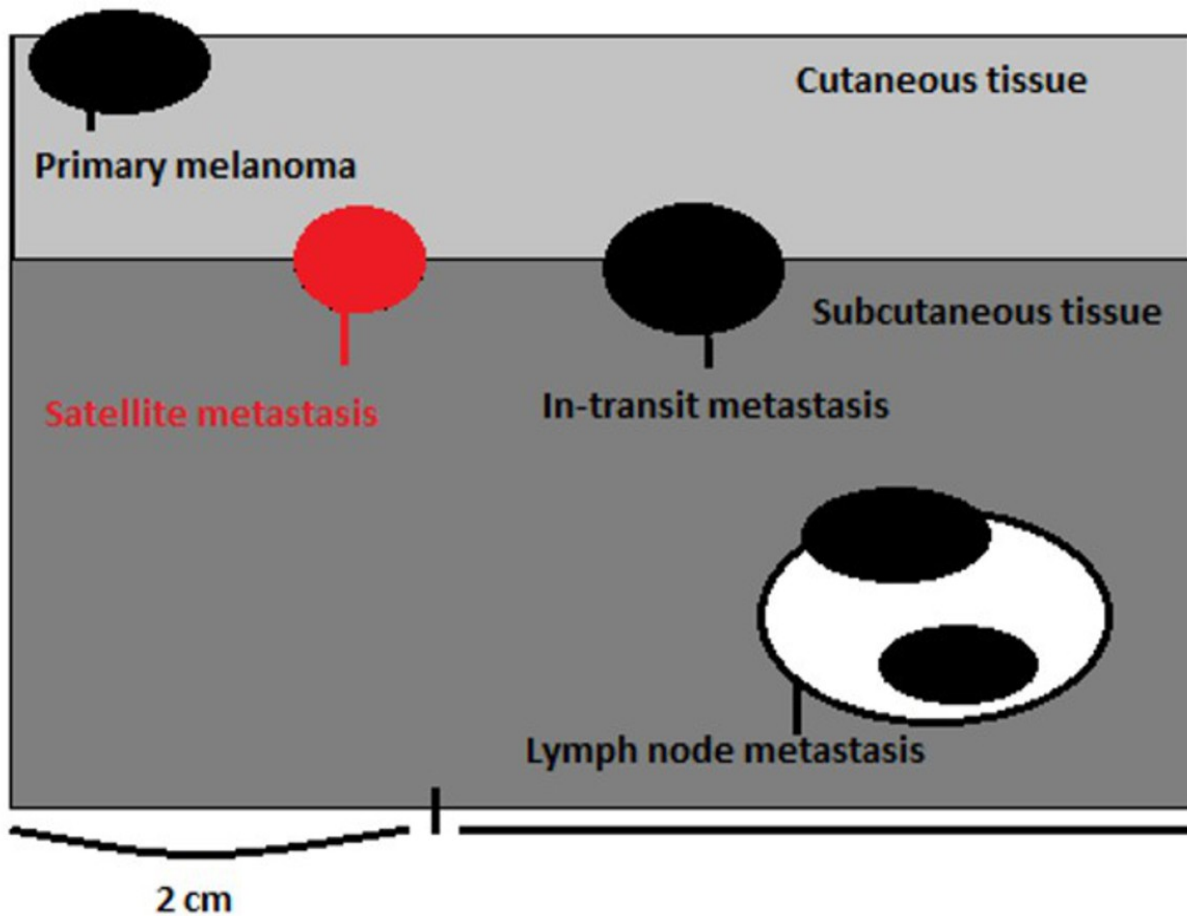


Fig. 3: Schematic drawing of locoregional metastasis. Satellite metastasis (red) are cutaneous or subcutaneous metastasis located between the primary lesion or scar tissue and the draining lymph node basin. They are located within 2 cm from the primary tumor or scar tissue. Satellite metastasis are considered a nodal metastasis in the TNM classification.

© Department of Radiology, University Hospital Antwerp - Antwerp/BE

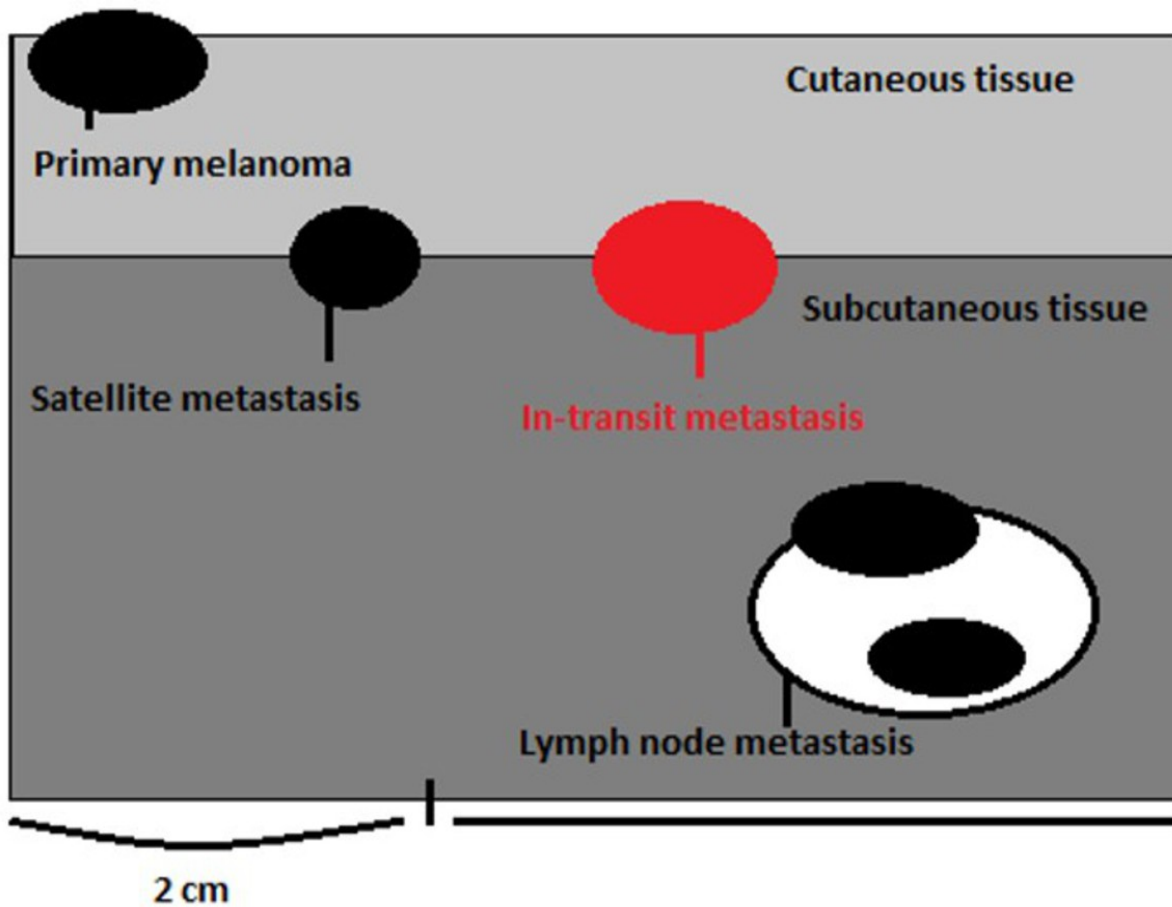


Fig. 4: Schematic drawing of in-transit metastasis. In-transit metastasis (red) are cutaneous or subcutaneous metastasis located between the primary lesion or scar tissue and the draining lymph node basin. They are 2 cm away from the primary tumor or scar and before reaching the regional lymph node basin. In-transit metastasis are considered a nodal metastasis in the TNM classification.

© Department of Radiology, University Hospital Antwerp - Antwerp/BE

Findings and procedure details

I. MERIT OF EACH IMAGING TECHNIQUE IN THE EVALUATION OF METASTATIC SPREAD OF MELANOMA

1. General need for imaging
2. Ultrasound
3. Radiography
4. Computed tomography
5. Magnetic resonance imaging
6. Lymphoscintigraphy
7. Positron emission tomography - computed tomography

II. POTENTIAL PATTERNS AND LOCATION OF DISTANT DISSEMINATION OF MELANOMA

1. Locoregional metastasis
2. Chest
3. Central nervous system
4. Abdomen
5. Musculoskeletal system
6. Miscellaneous

I. MERIT OF EACH IMAGING TECHNIQUE IN THE EVALUATION OF METASTATIC SPREAD OF MELANOMA

1. General need for imaging

Clinical Staging				Pathologic staging			Imaging recommendations asymptomatic patients
	OTis	NO	M0	T	N	M	
IA	T1a	NO	M0	IA	T1a	NO	M0
IB	T1b	NO	M0	IB	T1b	NO	M0
	T2a	NO	M0		T2a	NO	M0
IIA	T2b	NO	M0	IIA	T2b	NO	M0
	T3a	NO	M0		T3a	NO	M0
IIB	T3b	NO	M0	IIB	T3b	NO	M0
	T4a	NO	M0		T4a	NO	M0
IIC	T4b	NO	M0	IIC	T4b	NO	M0
III	Any T	N>NO	M0	IIIA	T1-4a	N1a	M0
					T1-4a	N2a	M0
				IIIB	T1-4b	N1a	M0
					T1-4b	N2a	M0
					T1-4a	N1b	M0
					T1-4a	N2b	M0
					T1-4a	N2c	M0
				IIIC	T1-4b	N1b	M0
					T1-4b	N2b	M0
					T1-4b	N2c	M0
					Any T	N3	M0
IV	Any T	Any N	M1	IV	Any T	Any N	M1

Table 2: The red line indicates in which patients screening with imaging should be considered. Asymptomatic patients with IA-IIA disease do not need screening with imaging. Patients with at least stage IIB disease, imaging should be considered. These are patients with a primary tumor of 2,1-4 mm thickness with ulcerations (T3b) or patients with primary tumor of >4 mm thickness (T4a). It is recommended to screen with Chest-XR, CT and/or PET/CT every 3-12 months and annual MRI of the brain during 2-5 years. After 5 year of follow-up, asymptomatic patients do not need any screening with imaging.

Table 2

References: Department of Radiology, University Hospital Antwerp - Antwerp/BE

2. Ultrasound

-Advantages:

- Cheap
- Primary melanoma
- Evaluation of local recurrence, in-transit or regional lymph nodes metastases [Fig. 5](#) on page 17
- Fine needle aspiration cytology (FNAC) [Fig. 6](#) on page 18 :
 - In-transit and satellite: 95% sensitivity and 100% specificity
 - Nodal basins: 79% sensitivity and 100% specificity

-Disadvantages:

- Limited use for distant metastasis

-Imaging characterization:

- Hypo-echoic [Fig. 7](#) on page 19
- Hypervascularisation on power doppler [Fig. 8](#) on page 20

3. Radiography

-Advantages:

- Cheap
- Low radiation dose
- Chest x-ray for baseline comparison [Fig. 9](#) on page 21

-Disadvantages:

- Low sensitivity and specificity
 - Bone metastasis only visible when cortical destruction or #30% trabecular bone loss occurs [Fig. 10](#) on page 22
- Limited role in staging/evaluation of metastatic melanoma

-Imaging characterization:

- Hilar enlargement [Fig. 11](#) on page 22
- Lung nodules or masses [Fig. 9](#) on page 21
- Bone metastasis are generally osteolytic [Fig. 10](#) on page 22

4. Computed tomography

-Advantages:

- Quick examination of large body parts
- Widespread availability
- Different windowing settings for the evaluation of bone and different organ systems on one examination [Fig. 12](#) on page 23
- Best technique detecting lung metastasis
- Monitoring treatment outcome: CT + serum LDH → predicting survival

-Disadvantages:

- Radiation dose
- Not the highest sensitivity and specificity in most organ systems

-Imaging characterization:

- Hypervascular metastasis
 - Enhancing on peak hepatic arterial phase [Fig. 13](#) on page 24
 - Heterogeneous, rim or nodular enhancement
- Hepatic metastasis
 - Multiphase CE CT with at least 2 different phases [Fig. 14](#) on page 25
- Intratumoral haemorrhage [Fig. 15](#) on page 25
 - Non CE CT and CE CT in acute setting
 - MRI when available

5. Magnetic resonance imaging

-Advantages:

- Detailed tumor size and preoperative assessment
- Highest sensitivity and specificity in most organ systems, except for lung metastasis
- Characterization questionable lesions
- Whole-body MRI promising technique

-Disadvantages:

- Limited availability
- Limited field of view
- Patient-related contraindications

-MRI characterization:

- Paramagnetic effect of melanin with typical signal on T1- and T2-WI [Fig. 16](#) on page 26
 - Hyperintense on T1-WI
 - Hypointense on T2-WI
- Melanotic metastasis comprise 25 % of lesions: >10% melanin cells
- Amelanotic metastasis with non specific signal intensity [Fig. 17](#) on page 27
- Hypervascular metastasis with contrast behavior similar to CT [Fig. 18](#) on page 28 [Fig. 19](#) on page 28
- Intratumoral haemorrhage in 19% of brain metastasis [Fig. 29](#) on page 36 [Fig. 30](#) on page 37
 - Acute, subacute and chronic bleeding

6. Lymphoscintigraphy

- Sentinel node is the first lymph node or group of lymph nodes, draining the tumor
- Radioactive tracer

- Primary staging
- Considered in stage IA
- Should be performed in stage IB and II

7. Positron emission tomography - computed tomography

-Advantages:

- Metabolic function and high anatomic resolution [Fig. 20](#) on page 30
- High specificity and sensitivity
- Characterization of indeterminate lesions [Fig. 21](#) on page 30
- Exact staging for patients with resectable distant metastasis

-Disadvantages:

- Expensive
- High radiation dose
- Limited availability

-PET alone has a poor anatomic resolution and low specificity and is not routinely used in metastatic melanoma

II. POTENTIAL PATTERNS AND LOCATION OF DISTANT DISSEMINATION OF MELANOMA

Metastatic pattern of malignant melanoma

Table 3

References: Department of Radiology, University Hospital Antwerp - Antwerp/BE

Metastatic pattern	Literature	Our data
1. Locoregional metastasis		
-Regional lymph nodes	59%	83%
-Lung	36%	20%
-Clinical examination		
-US and subsequent FNAC if indicated	20%	14%
-CT and MRI not routinely used		
-Liver	20%	8%
-Locations:	17%	8%

Table 2: This table shows a comparison between literature data and our data of the most common sites of metastasis in melanoma.

- Local recurrences
- Satellite metastasis Fig. 20 on page 32
- In-transit metastasis Fig. 23 on page 32
- Nodal basin

2. Chest

-CT modality of choice

-Lung is most affected visceral organ (36%)

-Most lesions measure 1-2 cm

-Feeding vessel as sign of hematogenous spread

-Location:

- Lung parenchyma
- Pleura
- Mediastinal and hilar lymph nodes
[Fig. 24](#) on page 32

3. Central nervous system

-MRI modality of choice

-Acute haemorrhagic brain metastasis: CT and CE CT [Fig. 29](#) on page 36 [Fig. 30](#) on page 37

-Locations:

- Brain: 20%
 - Intra-axial [Fig. 25](#) on page 33 [Fig. 26](#) on page 34
 - Leptomeningeal [Fig. 27](#) on page 35 [Fig. 28](#) on page 36
- Spinal:
 - Intramedullary
 - Leptomeningeal [Fig. 31](#) on page 38
 - Epidural [Fig. 17](#) on page 27

4. Abdomen

-Multiphasic CE CT [Fig. 14](#) on page 25

-MRI for questionable lesions

-Locations:

- Liver: 20%
 - Variable in size, up to 15 cm.
 - Intralesional hemorrhage, calcifications and necrotic areas [Fig. 32](#) on page 38

- Adrenal glands, usually unilateral [Fig. 33](#) on page 39
- Gastrointestinal tract: small bowel > colon > stomach [Fig. 34](#) on page 39
- Duodenum, rectum, esophagus and anus infrequent [Fig. 35](#) on page 40
- Spleen unfrequent [Fig. 36](#) on page 40
- Kidney, pancreas [Fig. 37](#) on page 41 and gallbladder [Fig. 38](#) on page 42 rare
- Lymph nodes [Fig. 39](#) on page 43

5. Musculoskeletal system

-CT for bone

-PET/CT or MRI for questionable lesions [Fig. 21](#) on page 30

-MRI for muscle

-Osteolytic, slightly expansile lesions [Fig. 10](#) on page 22

-Rarely isolated muscle involvement

-Location:

- Bone: 17%
 - Axial skeleton
 - Ribs
 - Others [Fig. 40](#) on page 43
- Muscles:
 - Lower extremities > trunk > upper extremities [Fig. 23](#) on page 32

6. Miscellaneous

- Although cardiac [Fig. 12](#) on page 23 and breast metastasis is rare, the prevalence is higher in melanoma compared to other tumors [Fig. 41](#) on page 43
- Salivary glands is extremely rare [Fig. 41](#) on page 43
- Primary melanoma of the eye and paranasal sinuses is known. Metastasis should be considered in disseminated disease, but metachronous tumor should always be considered

Images for this section:

Clinical Staging				Pathologic staging			Imaging recommendations asymptomatic patients	
	OTis	N0	M0	T	N	M		
IA	T1a	N0	M0	IA	T1a	N0	M0	No imaging for asymptomatic patients
IB	T1b	N0	M0	IB	T1b	N0	M0	
	T2a	N0	M0		T2a	N0	M0	
IIA	T2b	N0	M0	IIA	T2b	N0	M0	
	T3a	N0	M0		T3a	N0	M0	
IIB	T3b	N0	M0	IIB	T3b	N0	M0	
	T4a	N0	M0		T4a	N0	M0	
IIC	T4b	N0	M0	IIC	T4b	N0	M0	
III	Any T	N>N0	M0	IIIA	T1-4a	N1a	M0	
					T1-4a	N2a	M0	
				IIIB	T1-4b	N1a	M0	
					T1-4b	N2a	M0	
					T1-4a	N1b	M0	
					T1-4a	N2b	M0	
					T1-4a	N2c	M0	
				IIIC	T1-4b	N1b	M0	
					T1-4b	N2b	M0	
	T1-4b	N2c	M0					
				Any T	N3	M0		
IV	Any T	Any N	M1	IV	Any T	Any N	M1	

Table 2: The red line indicates in which patients screening with imaging should be considered. Asymptomatic patients with IA-IIA disease do not need screening with imaging. Patients with at least stage IIB disease, imaging should be considered. These are patients with a primary tumor of 2,1-4 mm thickness with ulcerations (T3b) or patients with primary tumor of >4 mm thickness (T4a). It is recommended to screen with Chest-XR, CT and/or PET/CT every 3-12 months and annual MRI of the brain during 2-5 years. After 5 year of follow-up, asymptomatic patients do not need any screening with imaging.

Table 2

© Department of Radiology, University Hospital Antwerp - Antwerp/BE

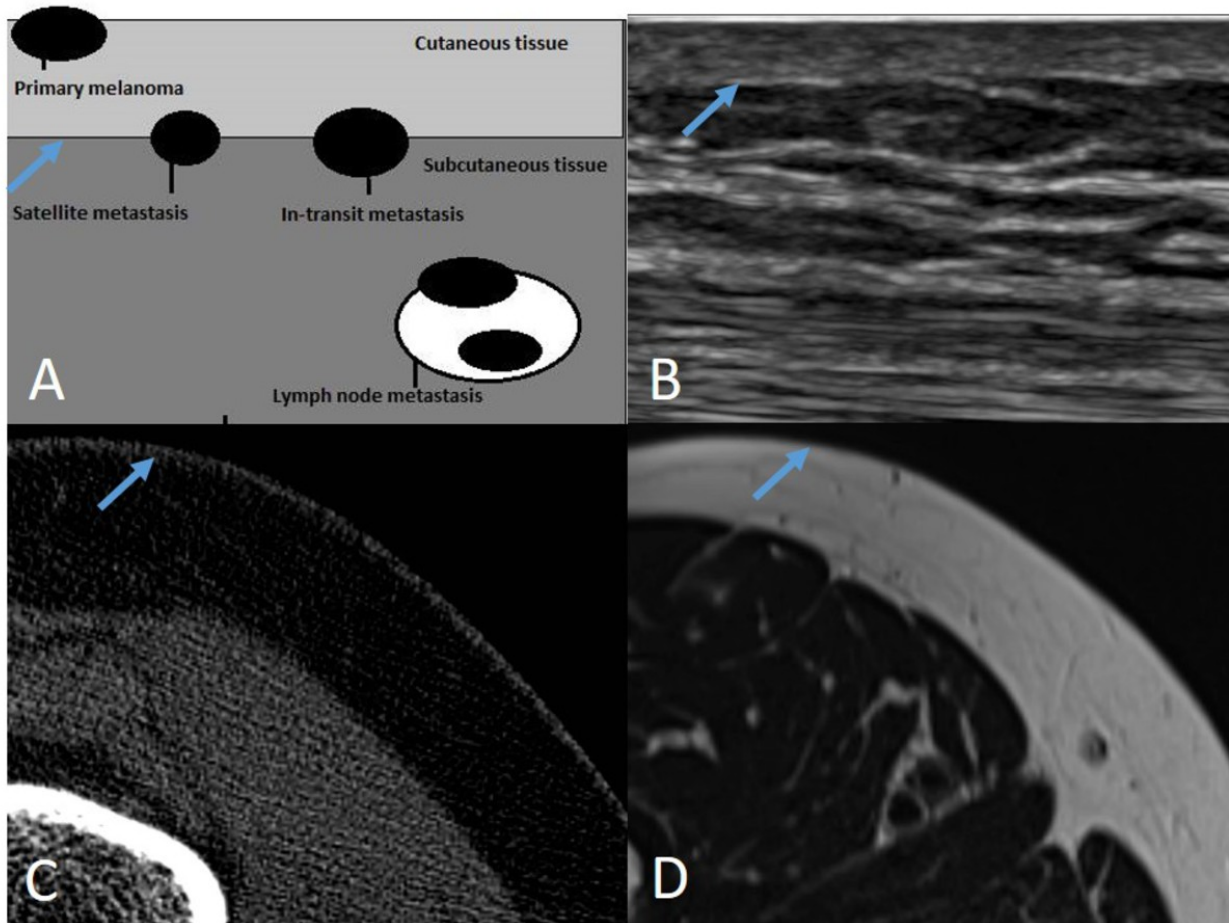


Fig. 5: Schematic drawing (A) of locoregional metastasis indicating the primary lesion, satellite metastasis, in-transit metastasis and metastasis to the nodal basin. An anatomical correlation with US (B), CT (C) and MRI (D) of the upper leg. The blue arrow indicates the transition between cutis and subcutis. US has a higher anatomical resolution of the cutis and subcutis than CT and MRI. Unfortunately, US is limited by its poor deep penetration.

© Department of Radiology, University Hospital Antwerp - Antwerp/BE

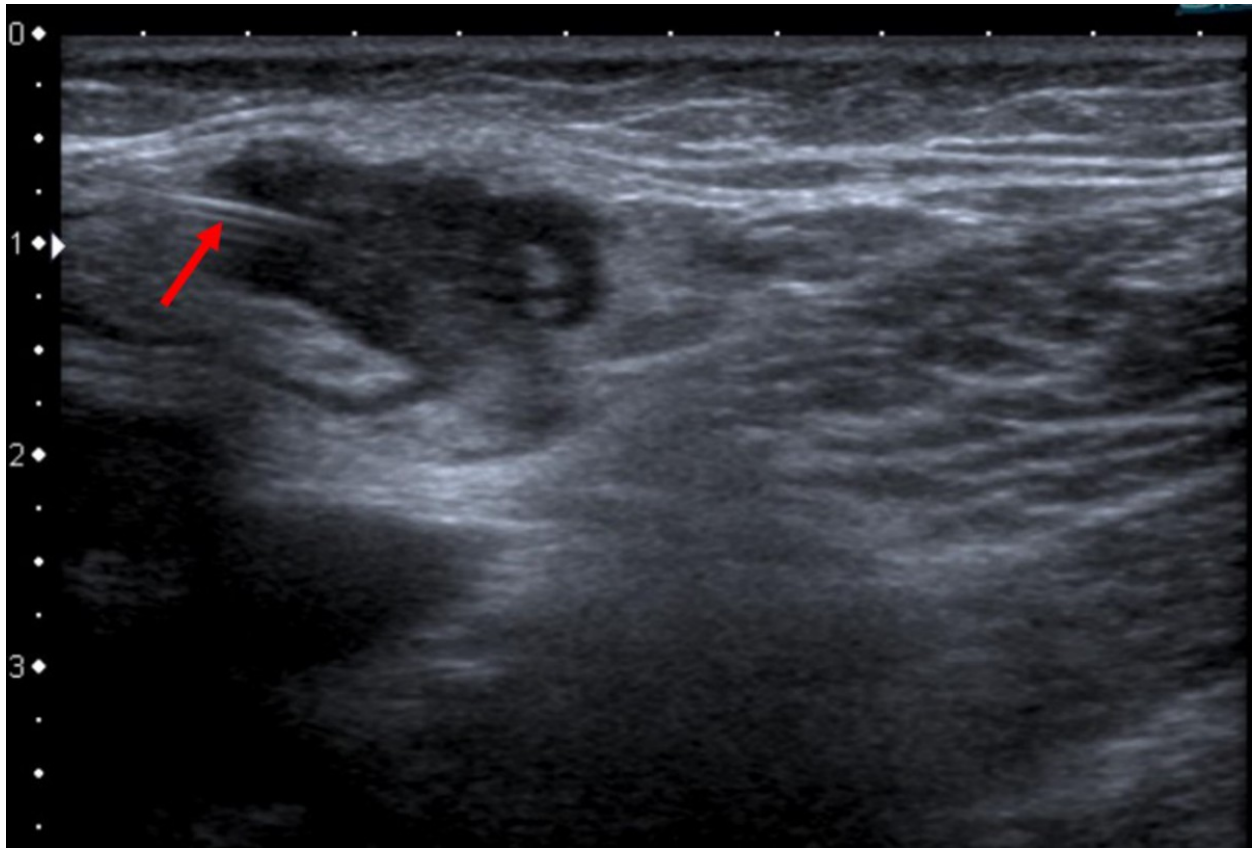


Fig. 6: US guided FNAC shows the needle (red arrow) in a hypo-echoic lesions. Histopathology confirmed metastatic melanoma.

© Department of Radiology, University Hospital Antwerp - Antwerp/BE

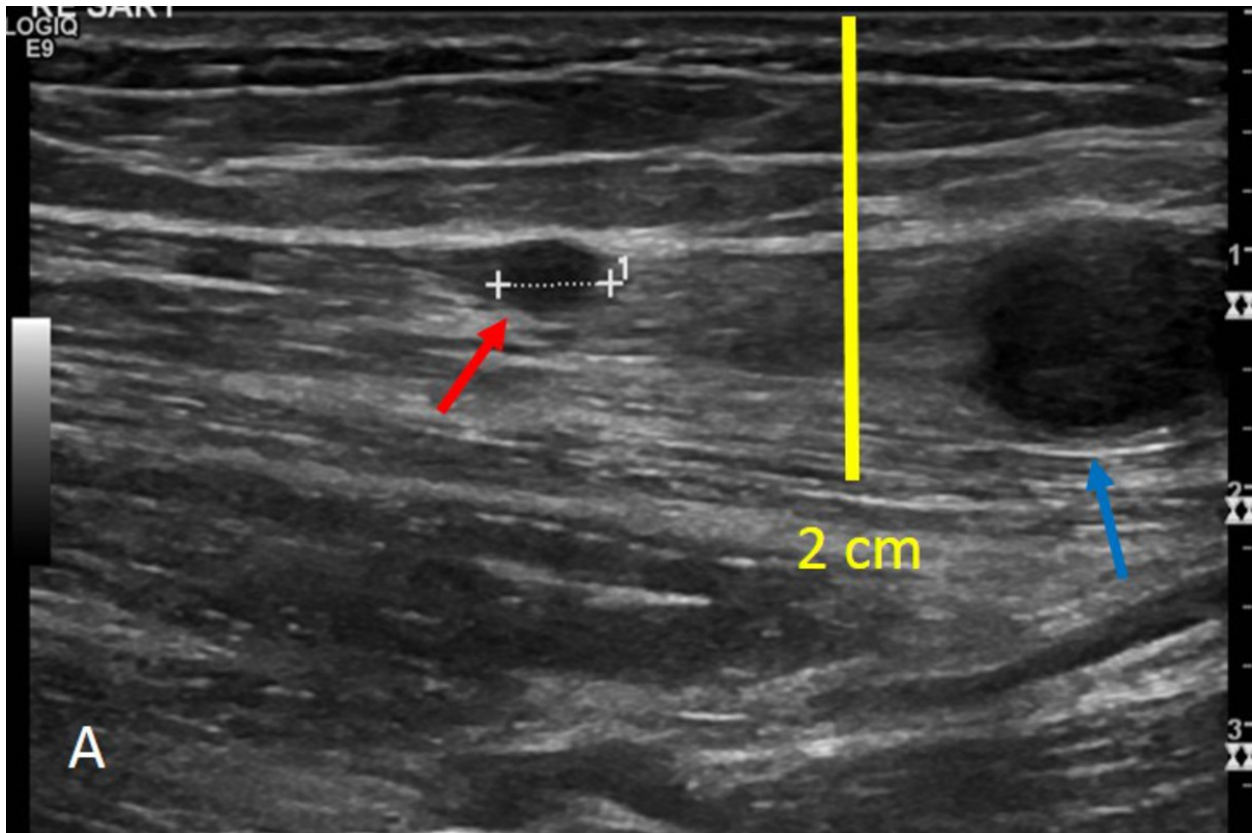


Fig. 7: Grey-scale US (A) of the left upper leg shows multiple hypoechoic lesions located in the sartorius muscle. The lesion indicated by the blue arrow is a satellite metastasis and the red arrow indicates an in-transit metastasis. The yellow line demarcates the difference between satellite and in-transit metastasis. The lesions have a cable-like appearance, initially interpreted as a neurogenic tumor. The lesions show increased vascularity on power doppler US (B).

© Department of Radiology, University Hospital Antwerp - Antwerp/BE

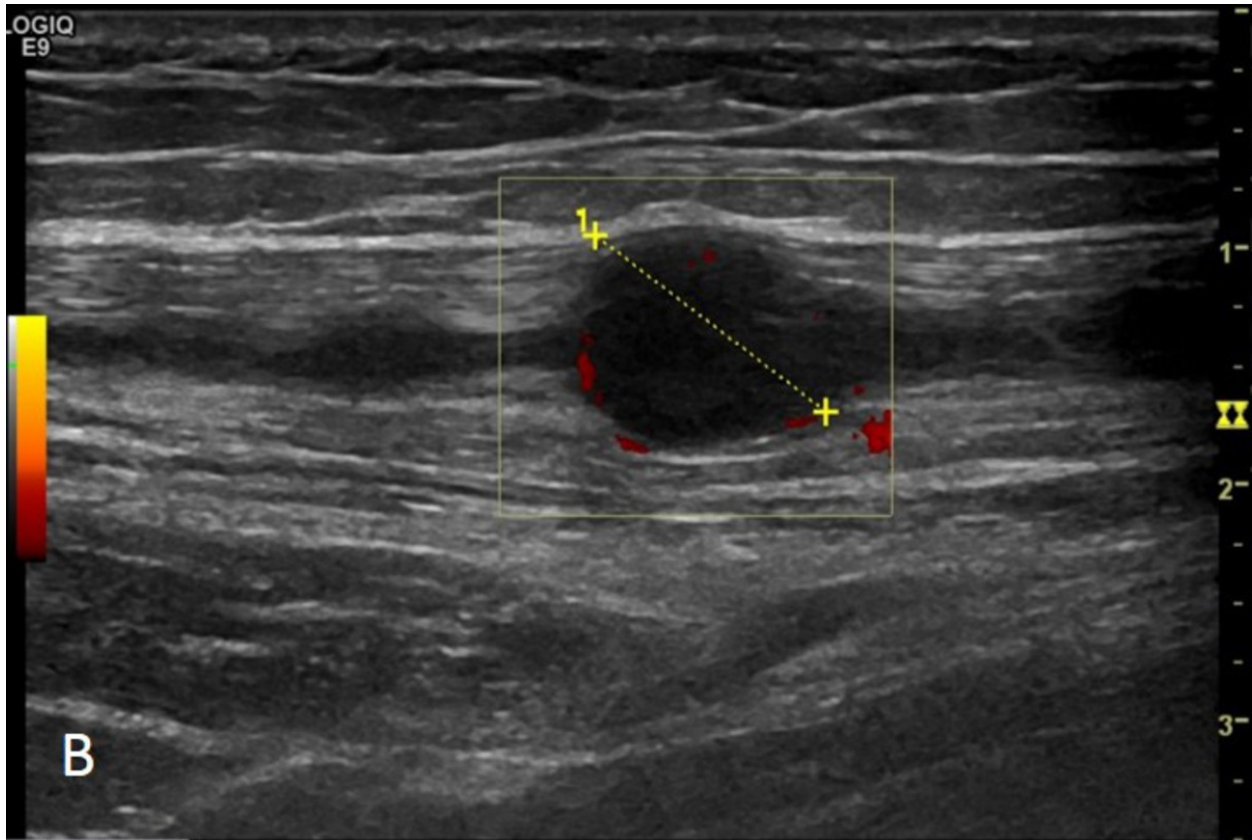


Fig. 8: Grey-scale US (A) of the left upper leg shows multiple hypoechoic lesions located in the sartorius muscle. The lesion indicated by the blue arrow is a satellite metastasis and the red arrow indicates an in-transit metastasis. The yellow line demarcates the difference between satellite and in-transit metastasis. The lesions have a cable-like appearance, initially interpreted as a neurogenic tumor. The lesions show increased vascularity on power doppler US (B).

© Department of Radiology, University Hospital Antwerp - Antwerp/BE

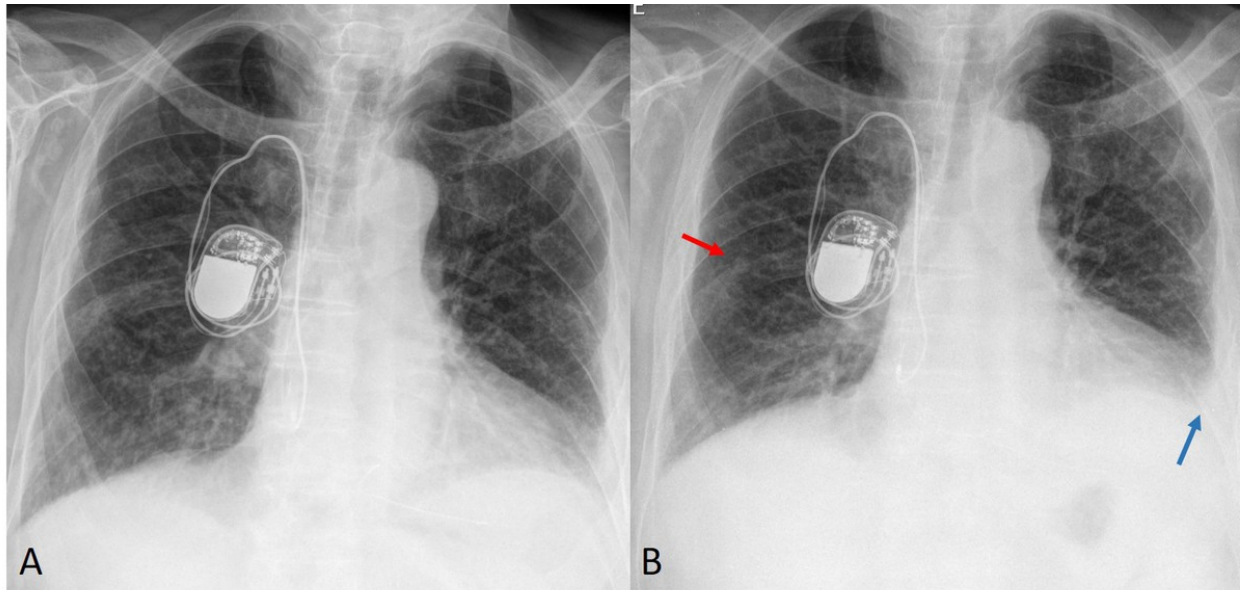


Fig. 9: A baseline X-ray of the chest (A), helps to detect small lung metastasis (red arrow) in the right lung and the pleural effusion in the left lung (blue arrow).

© Department of Radiology, University Hospital Antwerp - Antwerp/BE

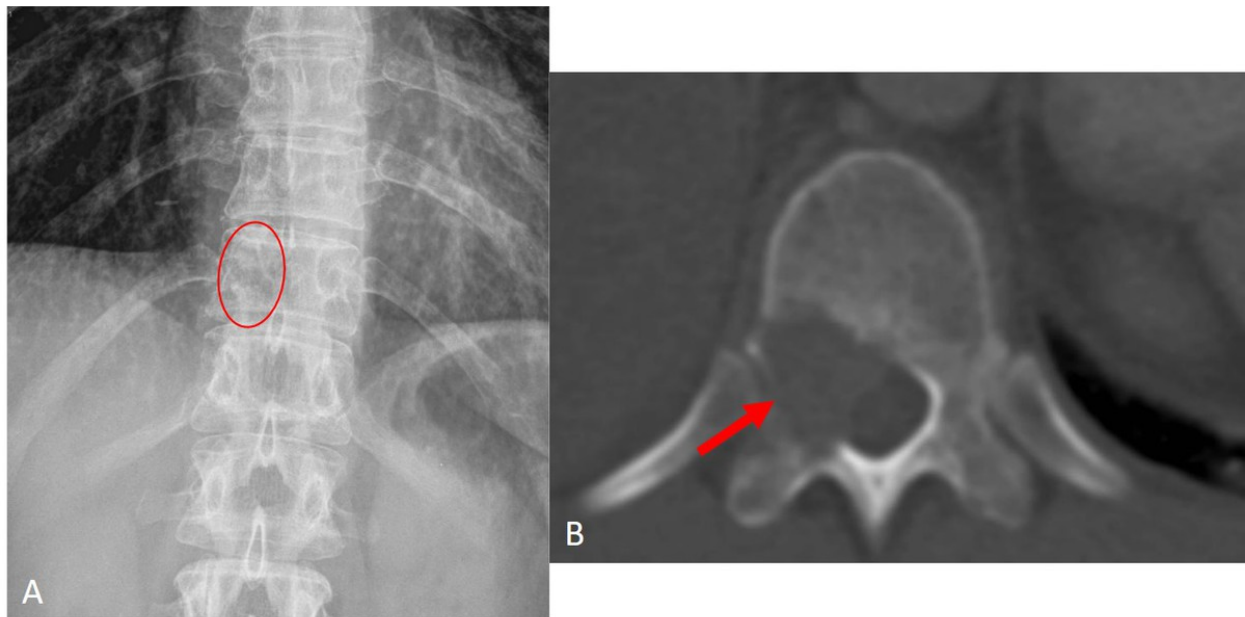


Fig. 10: Plain radiograph (A) shows destruction of the cortical outline of the pedicle of Th11 (red circle). CT (B) confirms a osteolytic metastasis with soft tissue component expanding in the spinal cord (red arrow).

© Department of Radiology, University Hospital Antwerp - Antwerp/BE

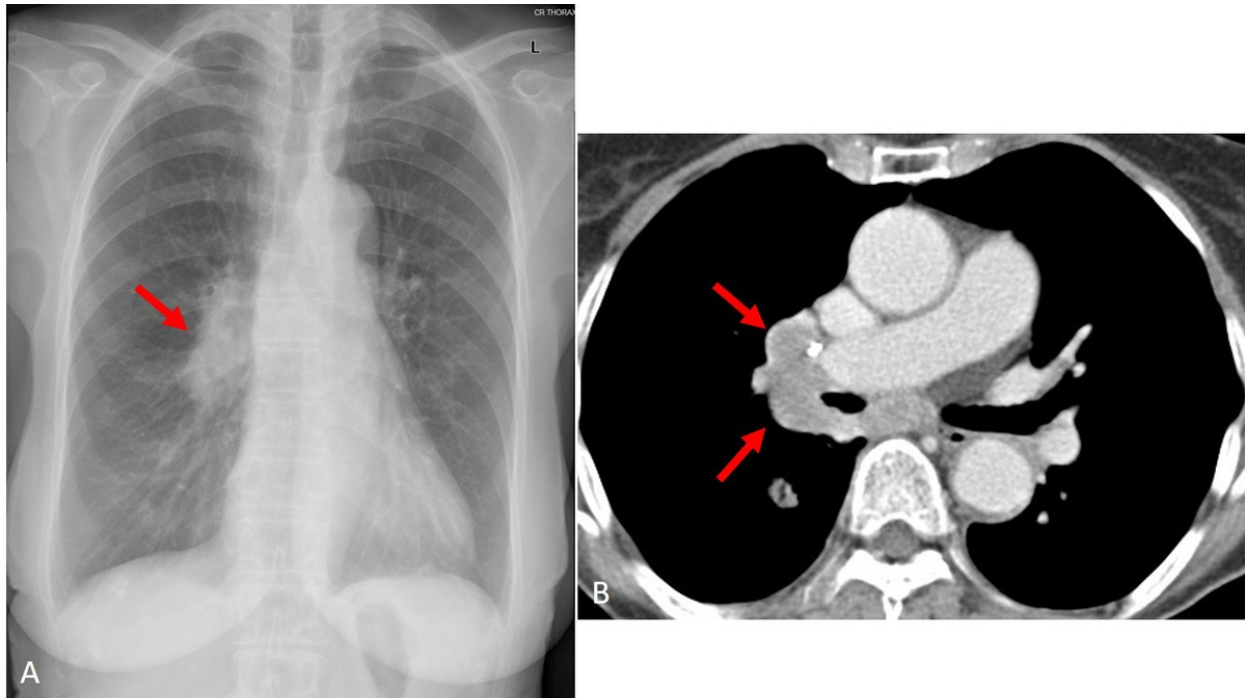


Fig. 11: PA chest X-ray (A) shows an enlarged right hilum (red arrow), suspicious for adenopathy which was confirmed on CE CT (B) (red arrows).

© Department of Radiology, University Hospital Antwerp - Antwerp/BE

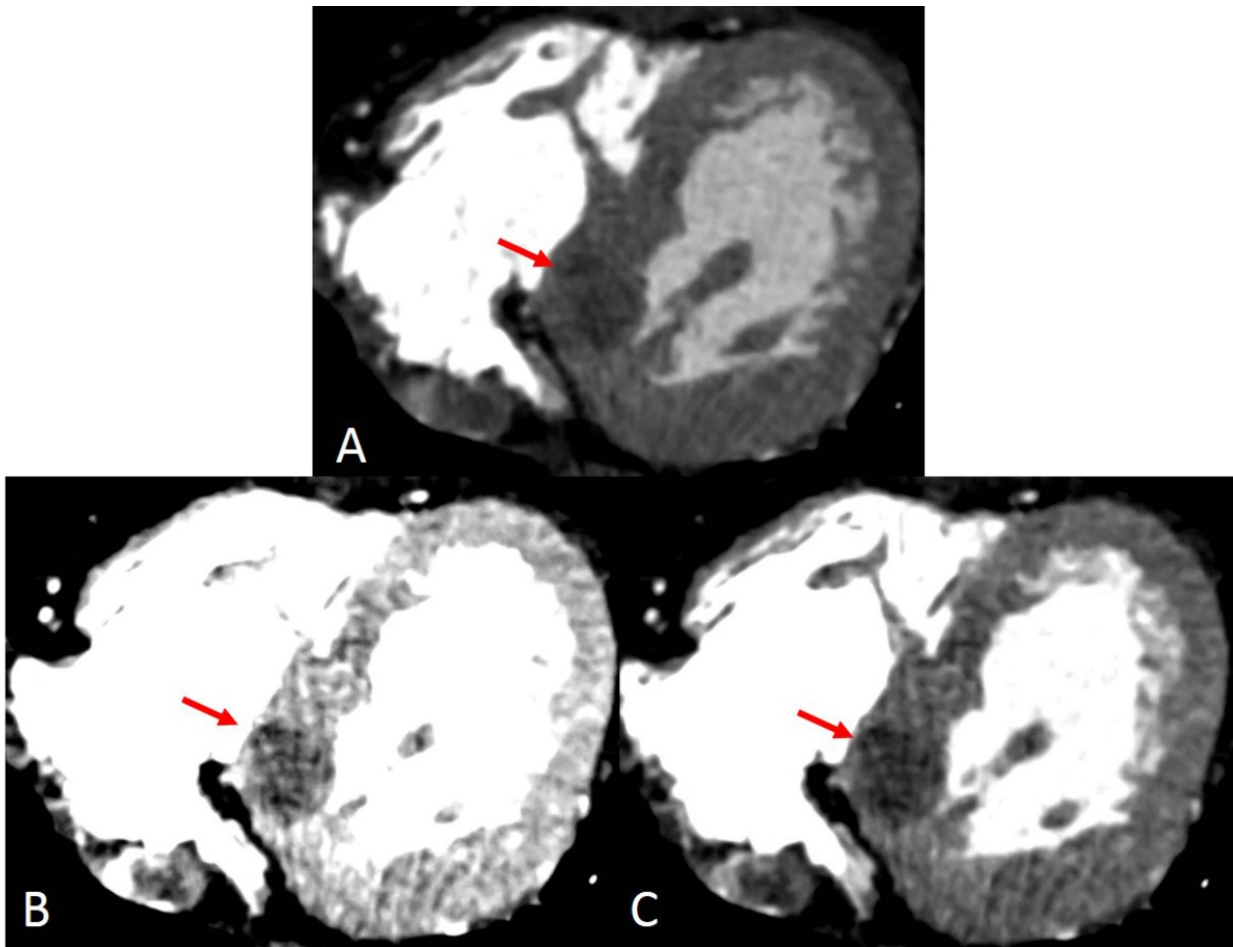


Fig. 12: Axial CE CT Chest. A, mediastinal window settings, shows a mass in the interventricular septum. Adjusting the window settings (B and C), allows a better visualisation of the mass.

© Department of Radiology, University Hospital Antwerp - Antwerp/BE

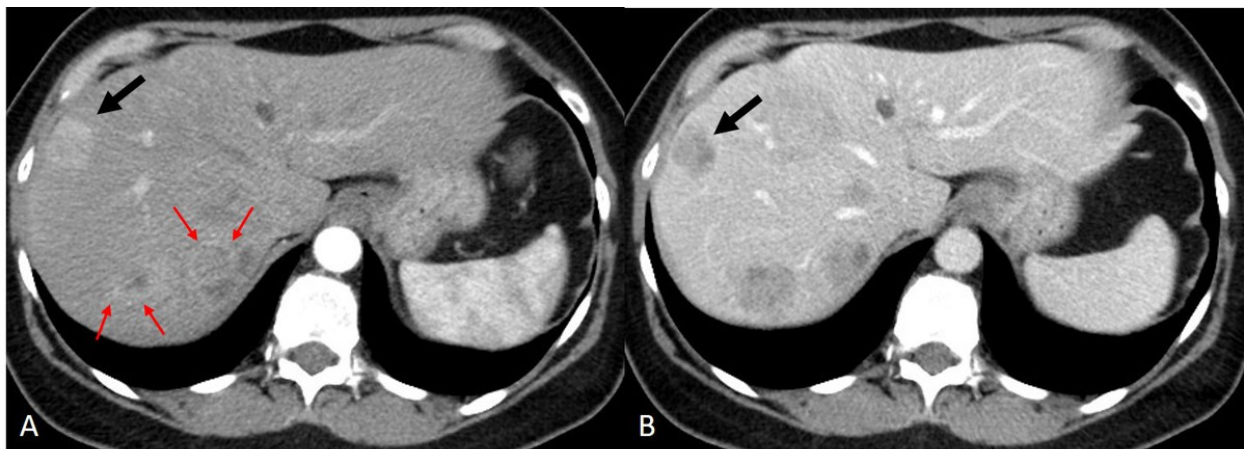


Fig. 13: CE CT arterial phase (A) and portovenous phase (B): A shows a lesion with enhancement in the arterial phase (black arrow) and washout in the portovenous phase. Two other lesions (red arrows) show peripheral rim enhancement in the arterial phase.

© Department of Radiology, University Hospital Antwerp - Antwerp/BE

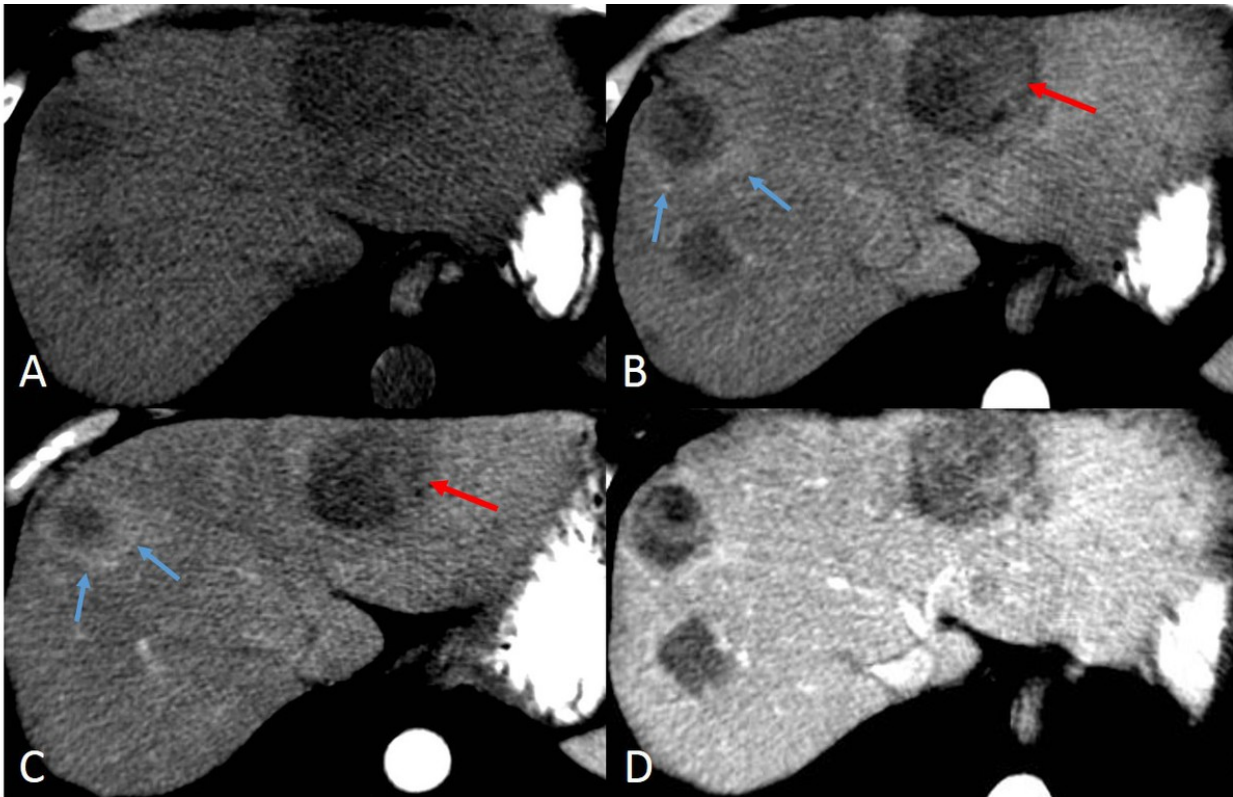


Fig. 14: Axial CT of the abdomen. Non-CE CT (A) shows multiple low attenuating liver masses. CE CT in the arterial phase (B and C), shows heterogeneous enhancement of a lesion (red arrow) as well as rim enhancement (blue arrow). CE CT in the portovenous phase (D), shows no washout.

© Department of Radiology, University Hospital Antwerp - Antwerp/BE

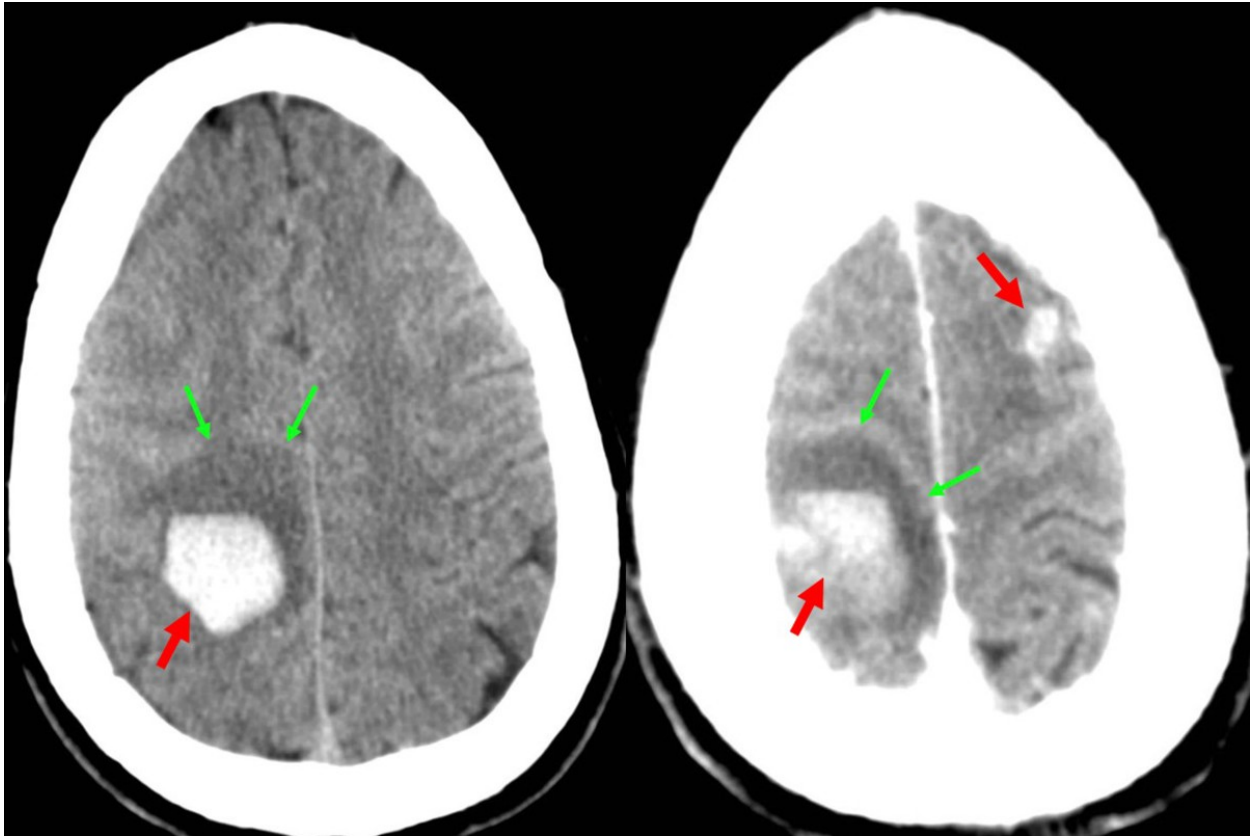


Fig. 15: Non CE CT shows a haemorrhagic lesion (red arrow) with peripheral edema (green arrows).

© Department of Radiology, University Hospital Antwerp - Antwerp/BE

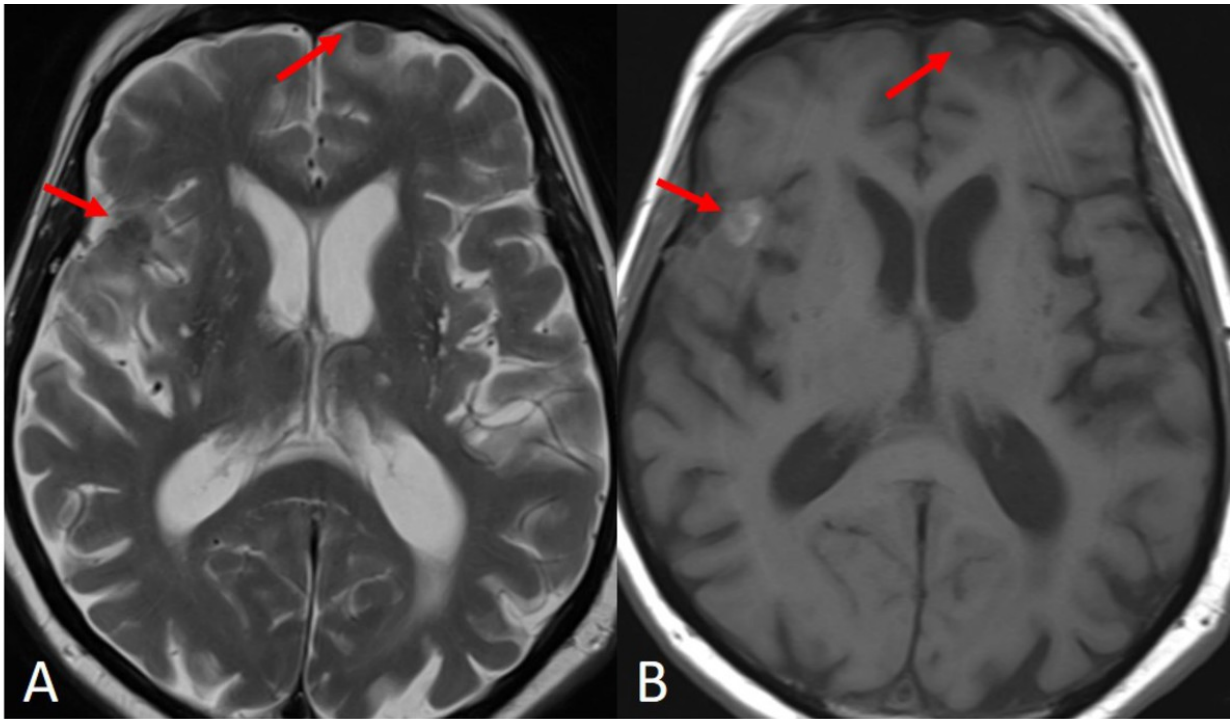


Fig. 16: An illustration of the specific behavior of metastatic melanoma within the brain on T1- and T2-WI. T2-WI (A) shows hypointense cortical nodules in the left frontal lobe and in the right temporal lobe (red arrows). The same lesions are hyperintense on T1-WI (B).

© Department of Radiology, University Hospital Antwerp - Antwerp/BE

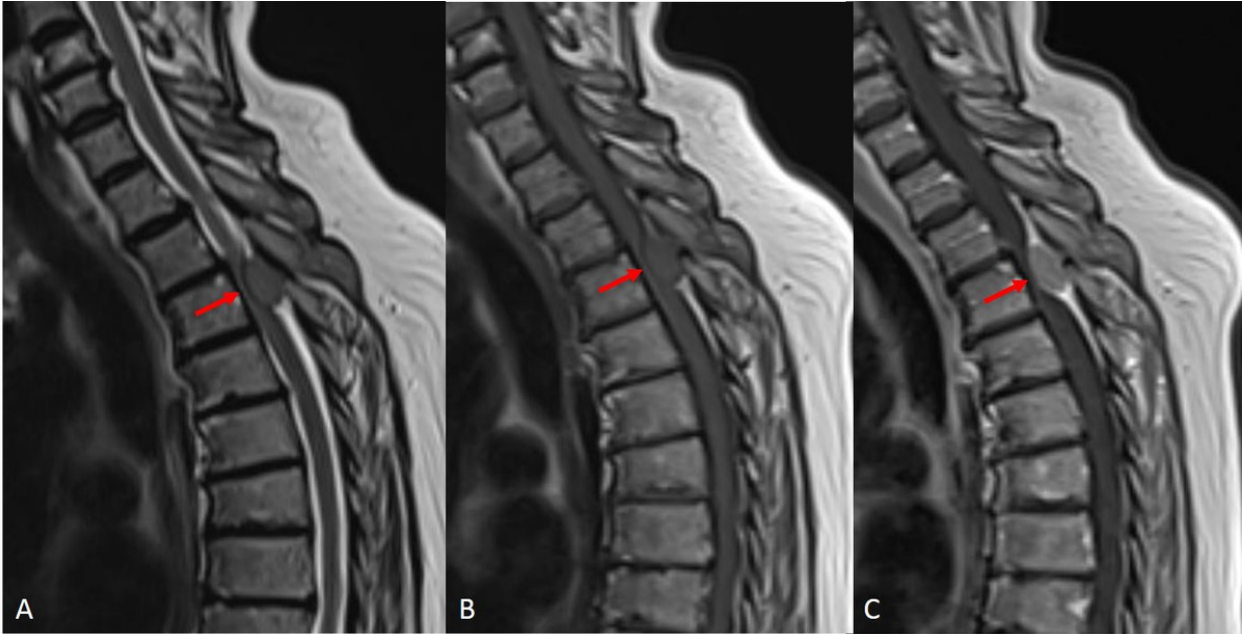


Fig. 17: T2-WI (A) and T1-WI (B) shows a lesion isointense to muscle posterior in the spinal canal , located in the epidural space (red arrow). T1-WI after gadolinium administration (C) shows marked enhancement. This is an example of metastatic melanoma with nonspecific signal characterization.

© Department of Radiology, University Hospital Antwerp - Antwerp/BE

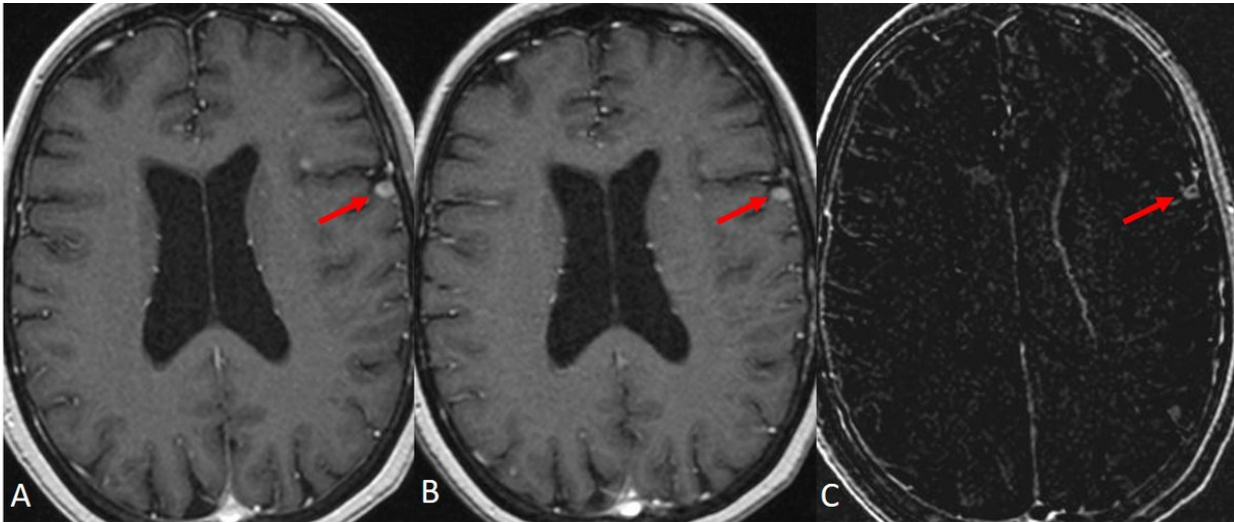


Fig. 18: T1 WI shows a spontaneous hyperintense leptomeningeal metastasis at the left Sylvian fissure. After gadolinium administration, there is a marked enhancement on T1 WI + Gd (B) and subtraction images (C).

© Department of Radiology, University Hospital Antwerp - Antwerp/BE

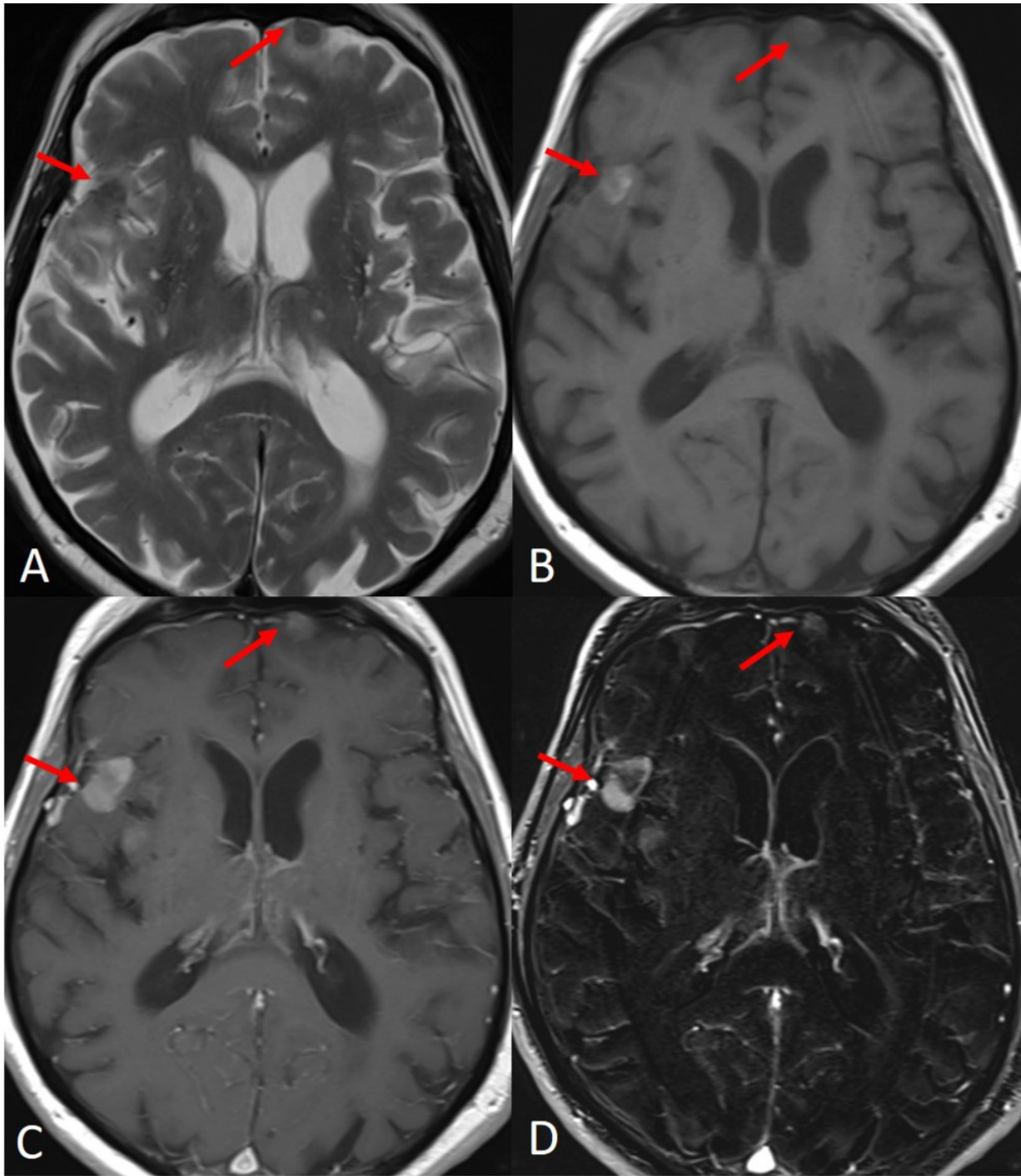


Fig. 19: An illustration of the specific behavior of metastatic melanoma within the brain on T1- and T2-WI. T2-WI (A) shows hypointense cortical nodules in the left frontal lobe and in the right temporal lobe (red arrows). The lesions are hyperintense on T1-WI (B). After administration of Gd contrast (C), there is marked enhancement seen on T1-WI and on the T1-WI subtraction images(D).

© Department of Radiology, University Hospital Antwerp - Antwerp/BE

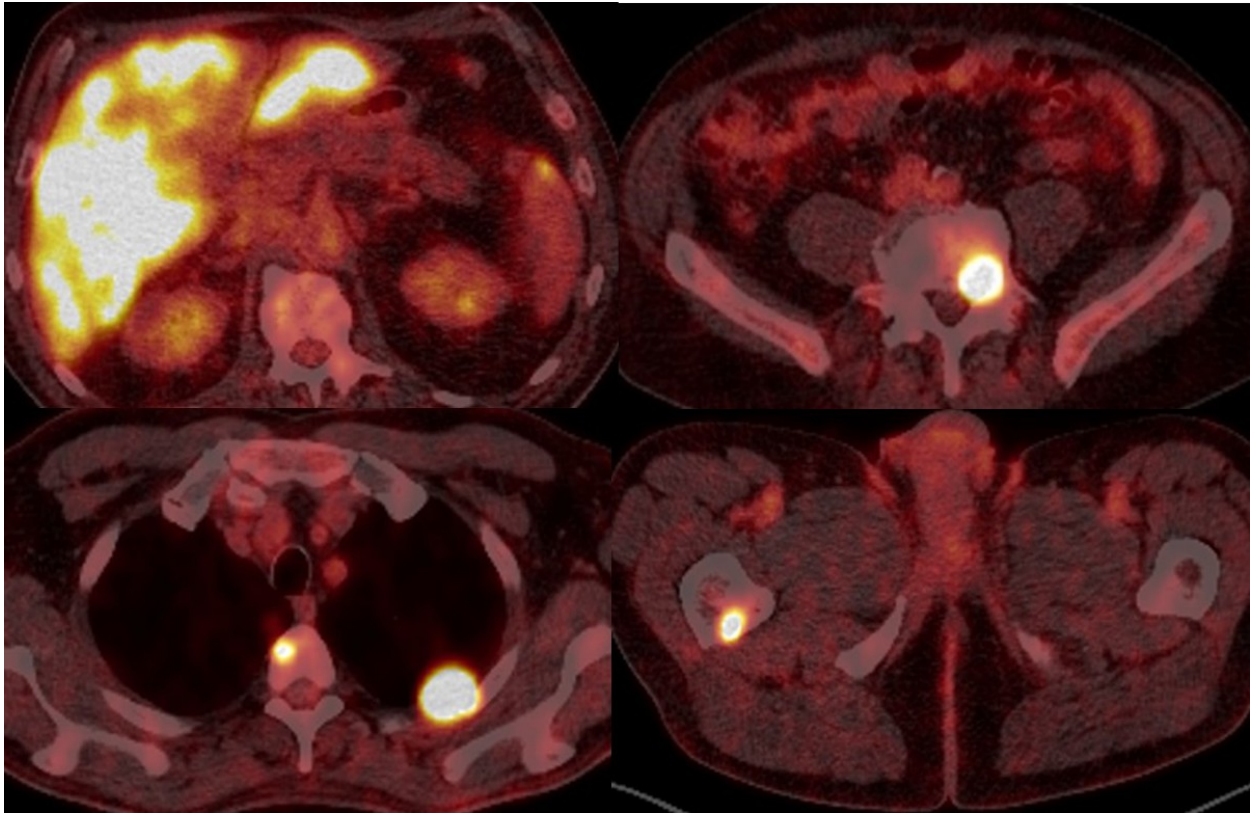


Fig. 20: Fusion PET/CT shows marked tracer hypercaptation in various locations in keeping with metastasis.

© Department of Radiology, University Hospital Antwerp - Antwerp/BE

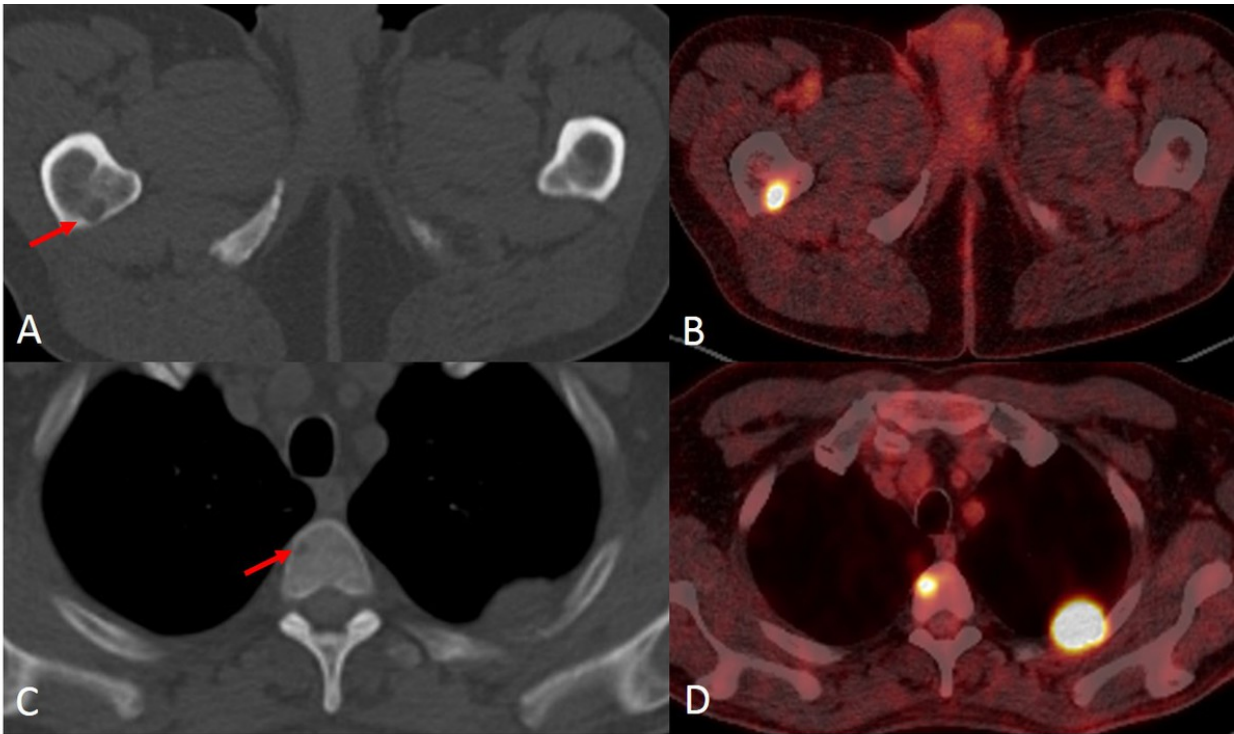


Fig. 21: Axial CT shows questionable lytic lesions in the right femoral neck (A) and in the thoracic spine (C). Fusion PET/CT (B and D) confirms metabolic activation, in this patient, in keeping with metastatic melanoma.

© Department of Radiology, University Hospital Antwerp - Antwerp/BE



Fig. 22: CE CT of the abdomen (A) shows an enhancing subcutaneous metastasis located in the right gluteal region (white arrow). Follow-up CE CT (B) shows a marked enlargement of the lesions (white arrow).

© Department of Radiology, University Hospital Antwerp - Antwerp/BE

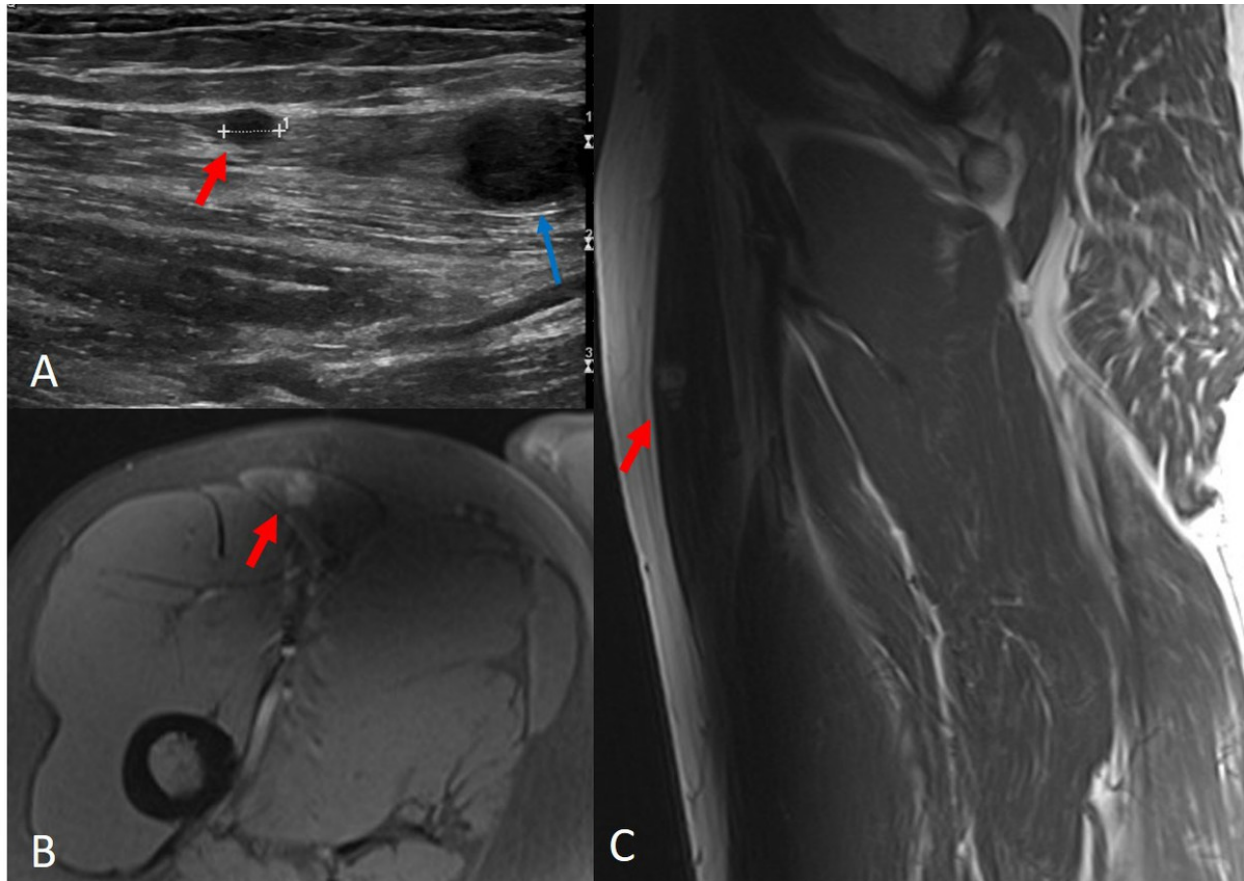


Fig. 23: Grey-scale US of the right upper leg (A) shows one satellite (blue arrow) and multiple in-transit metastases (red arrow) located in the sartorius muscle. Axial T1-WI with fs (B) and sagittal T1 WI (C) shows a spontaneous hyperintense nodular lesion in the sartorius muscle.

© Department of Radiology, University Hospital Antwerp - Antwerp/BE

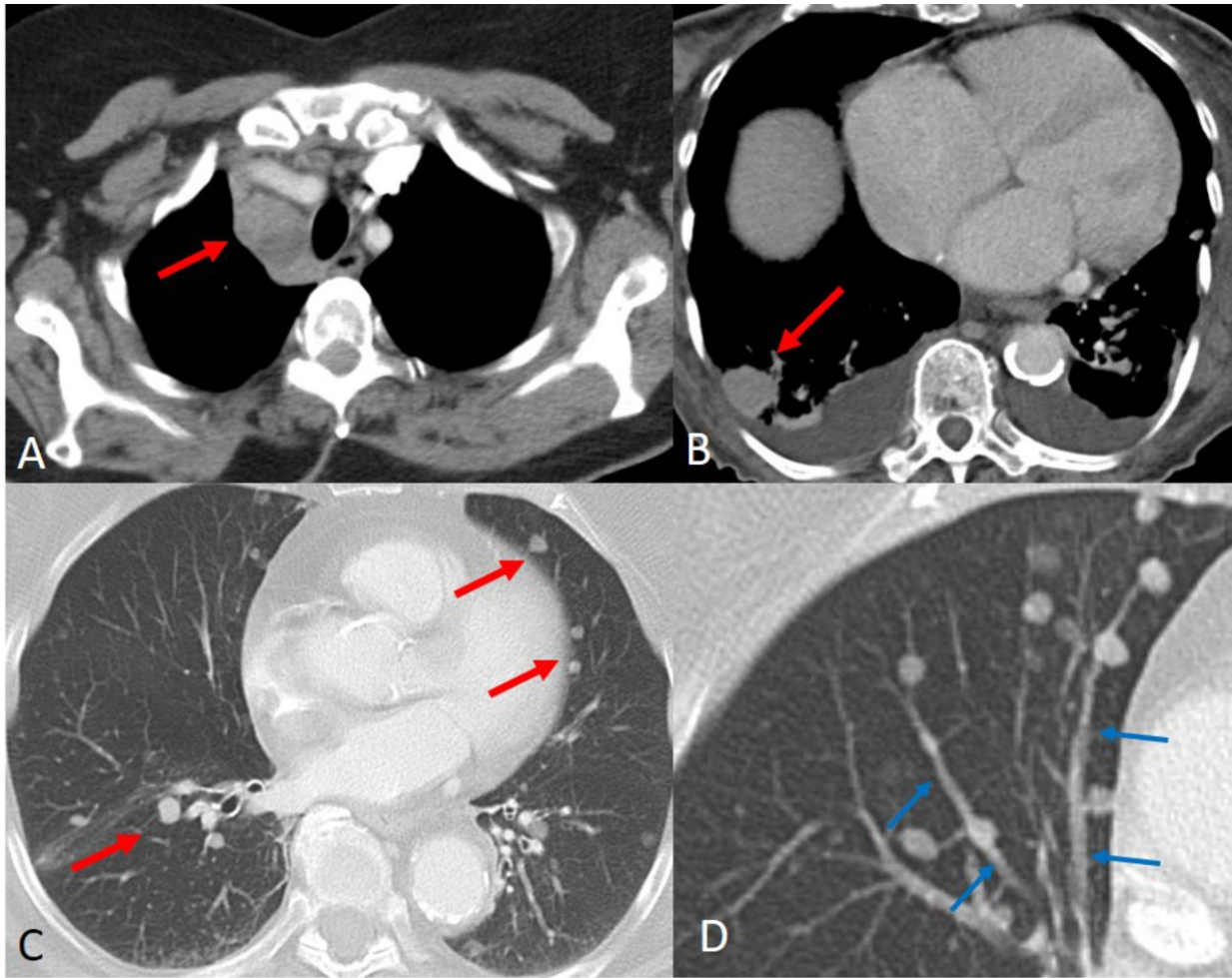


Fig. 24: CE CT of the chest of different patients shows mediastinal lymph node (A), pleural (B), multiple pulmonary (C) metastases. Illustration of feeding vessels (blue arrows), in keeping with hematogenous spread (D).

© Department of Radiology, University Hospital Antwerp - Antwerp/BE

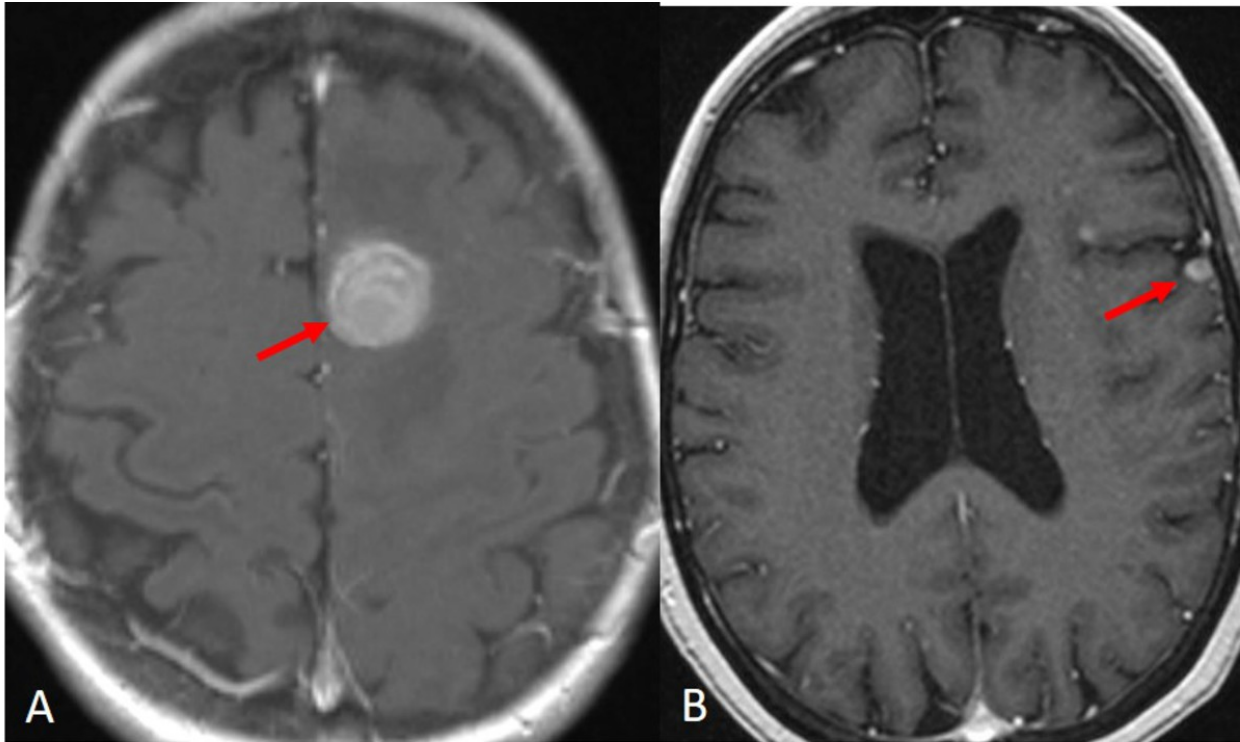


Fig. 25: Axial T1-WI after gd shows a cortical lesion in the frontal lobe (A) and a nodular leptomeningeal lesion posterior of the sylvian fissure (B).

© Department of Radiology, University Hospital Antwerp - Antwerp/BE

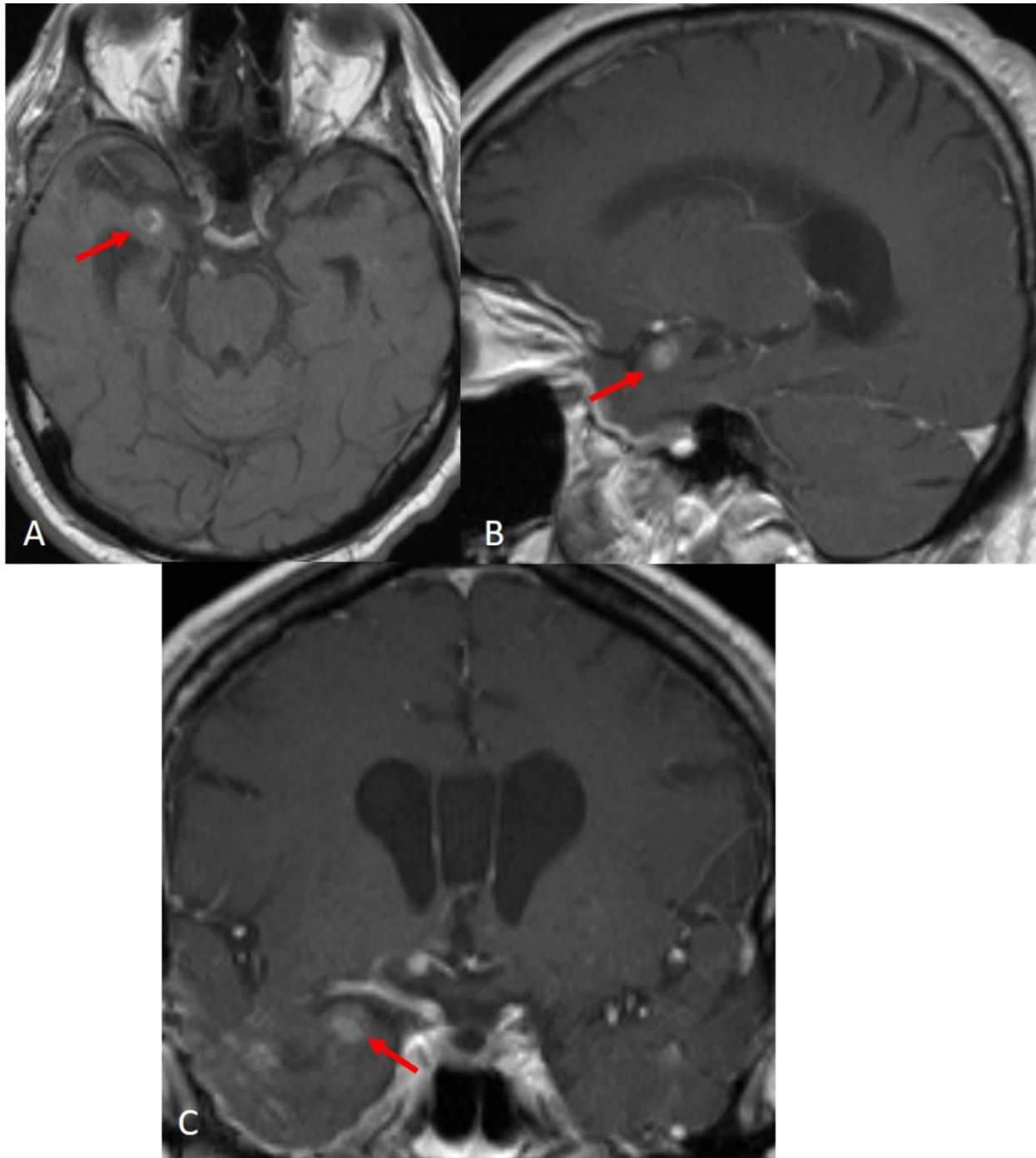


Fig. 26: Axial T1-WI (A) shows a spontaneous hyperintense lesion in the right hippocampus. Saggital (B) and coronal (C) T1-WI + gd clearly demonstrates the hippocampal localization.

© Department of Radiology, University Hospital Antwerp - Antwerp/BE

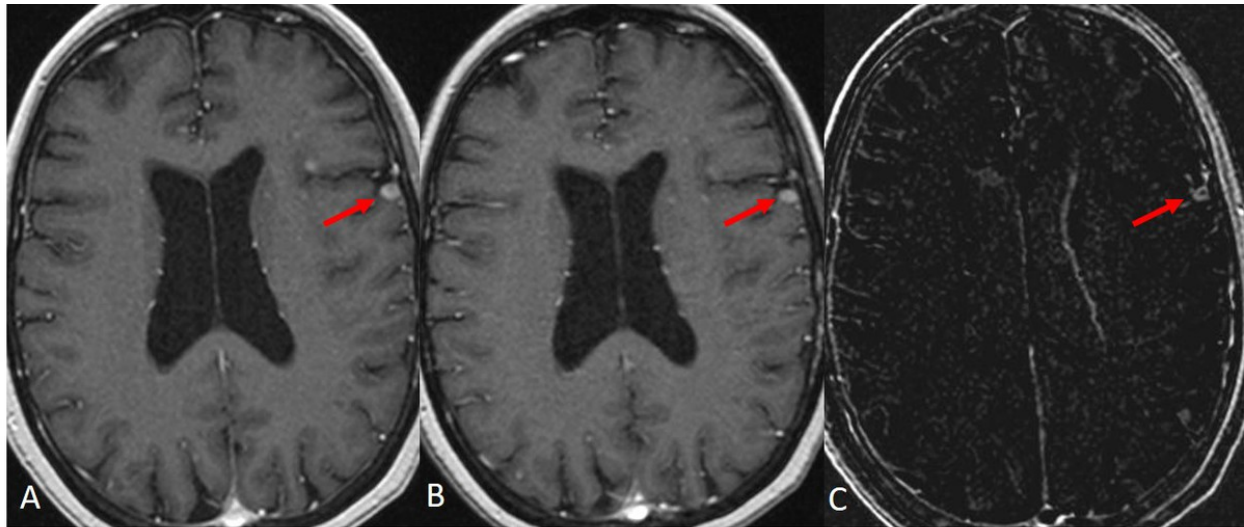


Fig. 27: T1 WI shows a spontaneous hyperintense leptomeningeal metastasis at the left Sylvian fissure. After gadolinium administration, there is a marked enhancement on T1 WI + Gd (B) and subtraction images (C).

© Department of Radiology, University Hospital Antwerp - Antwerp/BE

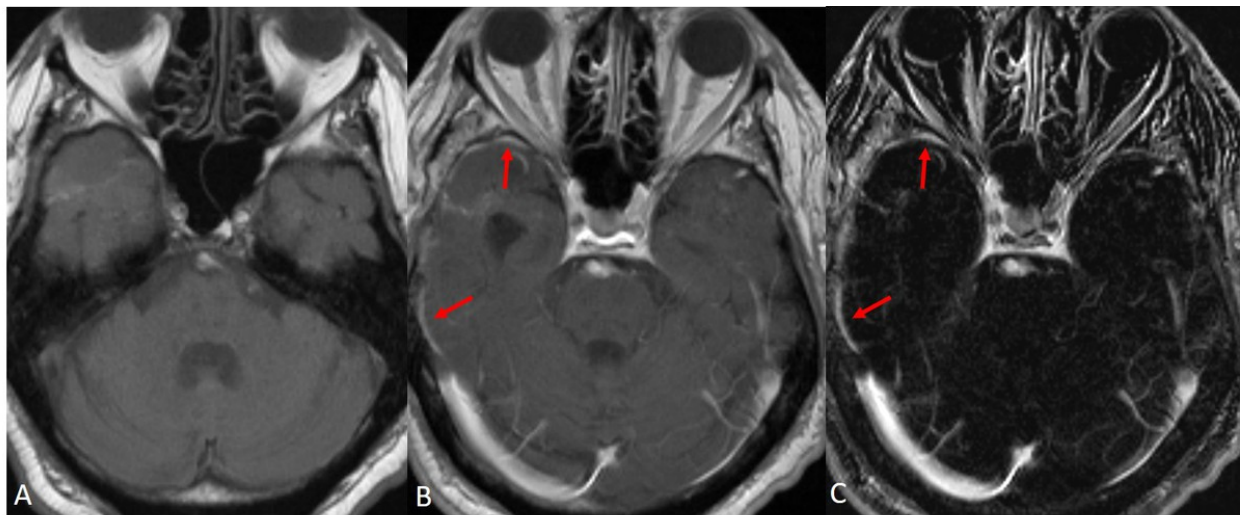


Fig. 28: Axial T1-WI before (A) and after administration of gadolinium (B) shows a diffuse enhancement (green arrows) of the leptomeninges of the right temporal lobe, which is clearly visible on the T1-WI subtraction images(C).

© Department of Radiology, University Hospital Antwerp - Antwerp/BE

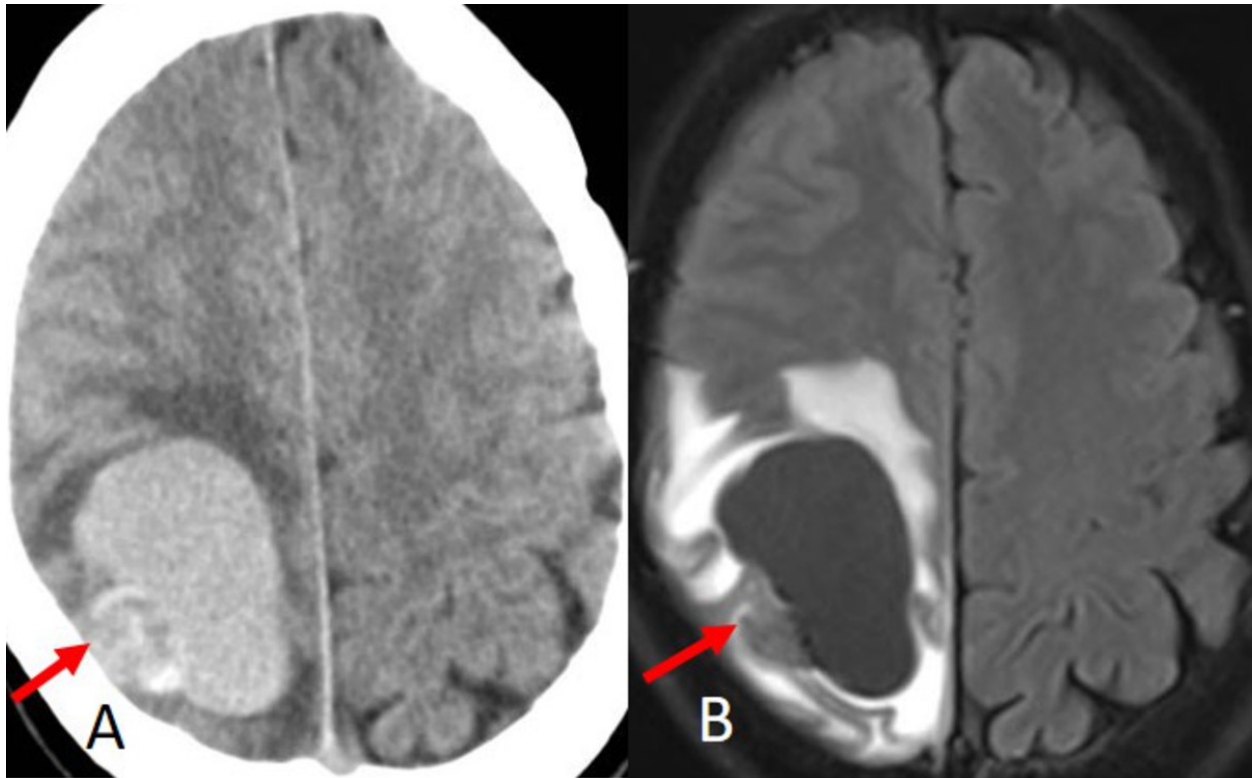


Fig. 29: CT and MRI of an acute intratumoral haemorrhage. Non-CE CT (A) shows a heterogeneous hyperdense lesion with associated haemorrhage and marked perilesional edema. T2-WI (B) confirms as a hypo- to isointense lesion with hyperintense surrounding edema. The haemorrhage is hypointense.

© Department of Radiology, University Hospital Antwerp - Antwerp/BE

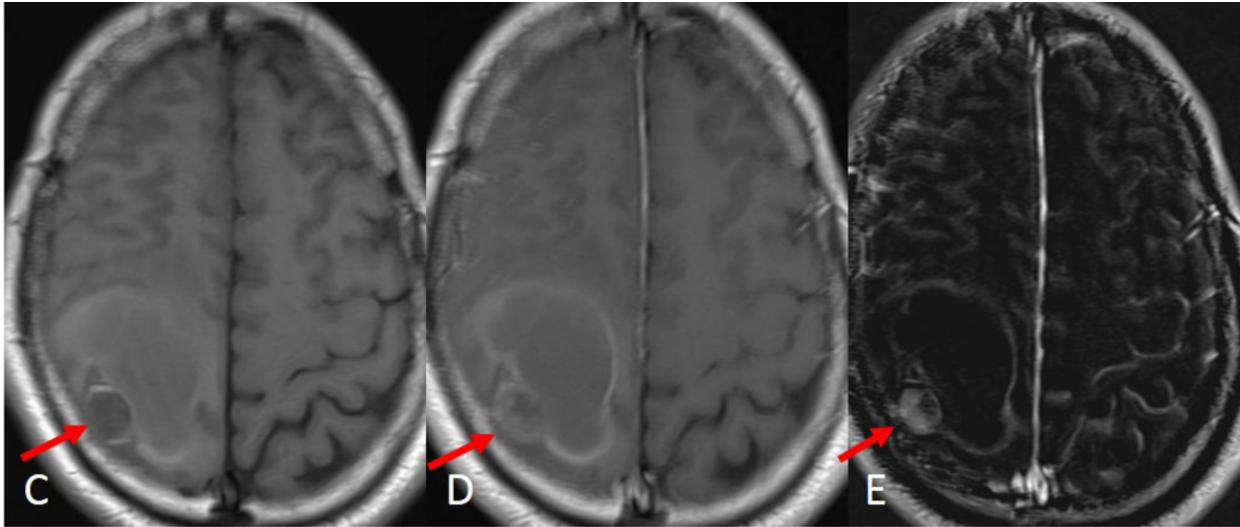


Fig. 30: T1-WI (C) shows a hypointense lesion with a peripheral hyperintense rim. The haemorrhage is hypo- to isointense. T1-WI after administration of gadolinium (D) shows heterogeneous and peripheral rim enhancement of the nodule and peripheral rim enhancement of the haemorrhage which is clearly seen on T1-WI subtraction images (E).

© Department of Radiology, University Hospital Antwerp - Antwerp/BE

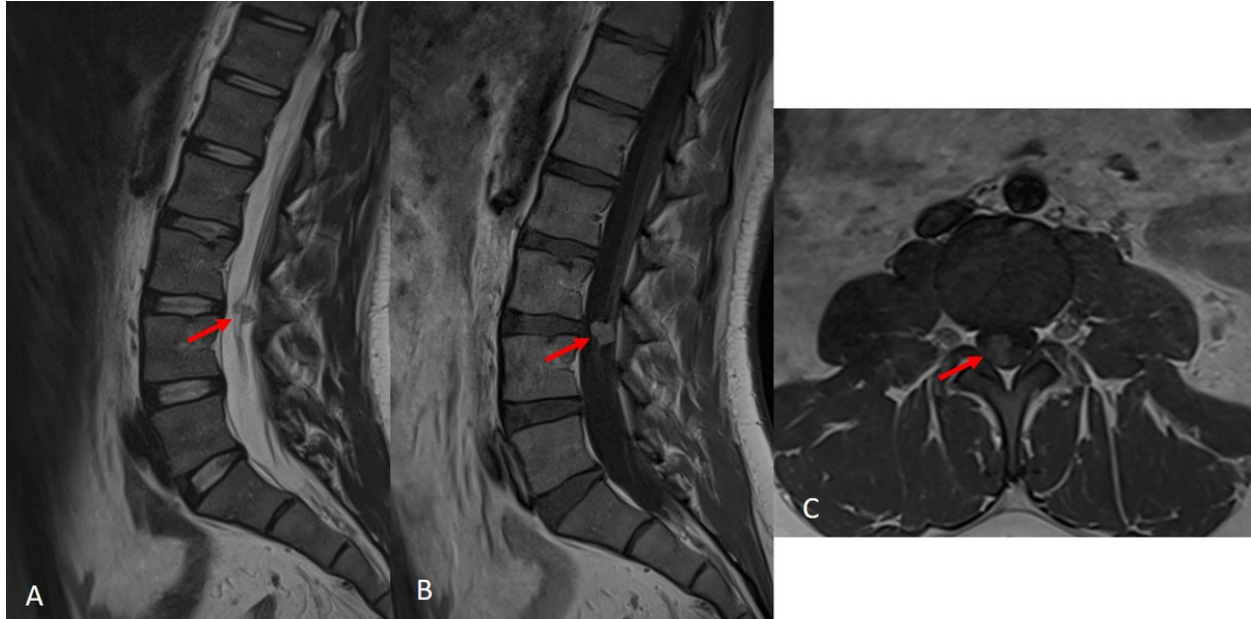


Fig. 31: T2-WI (A) shows an isointense leptomeningeal metastasis (red arrow) in the spinal cord, located at the cauda equina. Sagittal (B) and axial (A) contrast-enhanced T1-WI shows a marked enhancement (red arrow).

© Department of Radiology, University Hospital Antwerp - Antwerp/BE

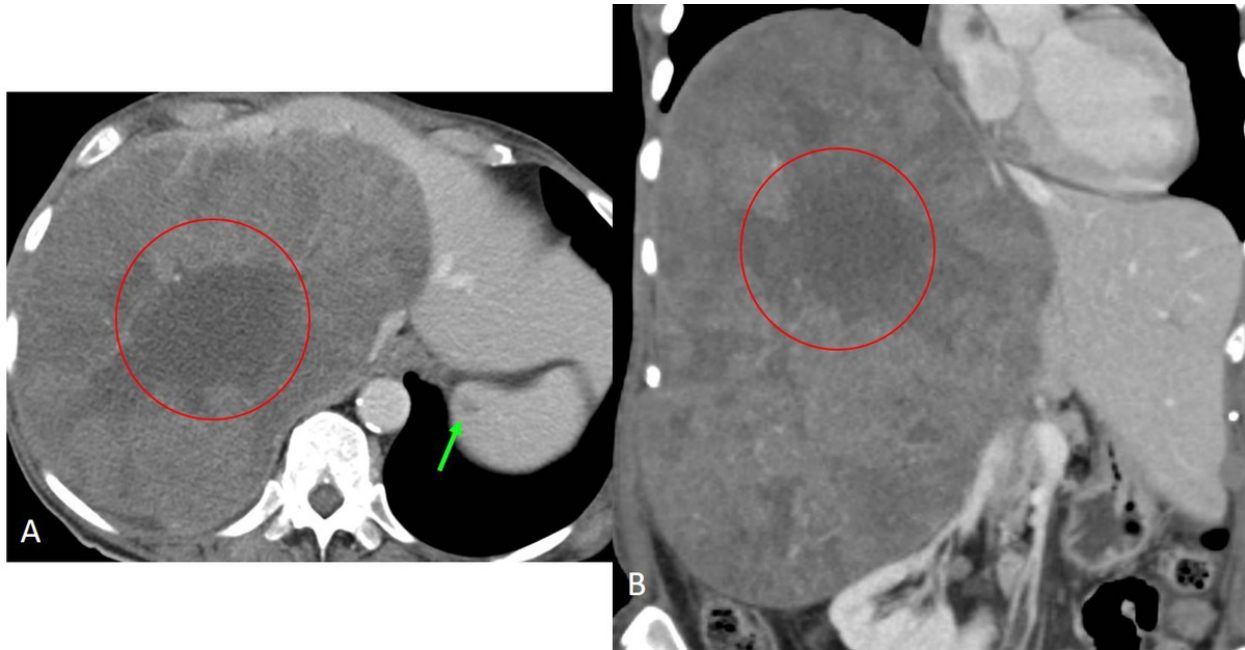


Fig. 32: Axial (A) and coronal (B) CE CT of the abdomen. A and B shows a large heterogeneous enhancing lesion in the liver. The lesion contains hypodense regions with no contrast enhancement in keeping with necrotic areas. The red circle indicates a large necrotic area. This patient had diffuse metastases with one large liver lesion. Mark the small metastasis in the spleen (green arrow).

© Department of Radiology, University Hospital Antwerp - Antwerp/BE

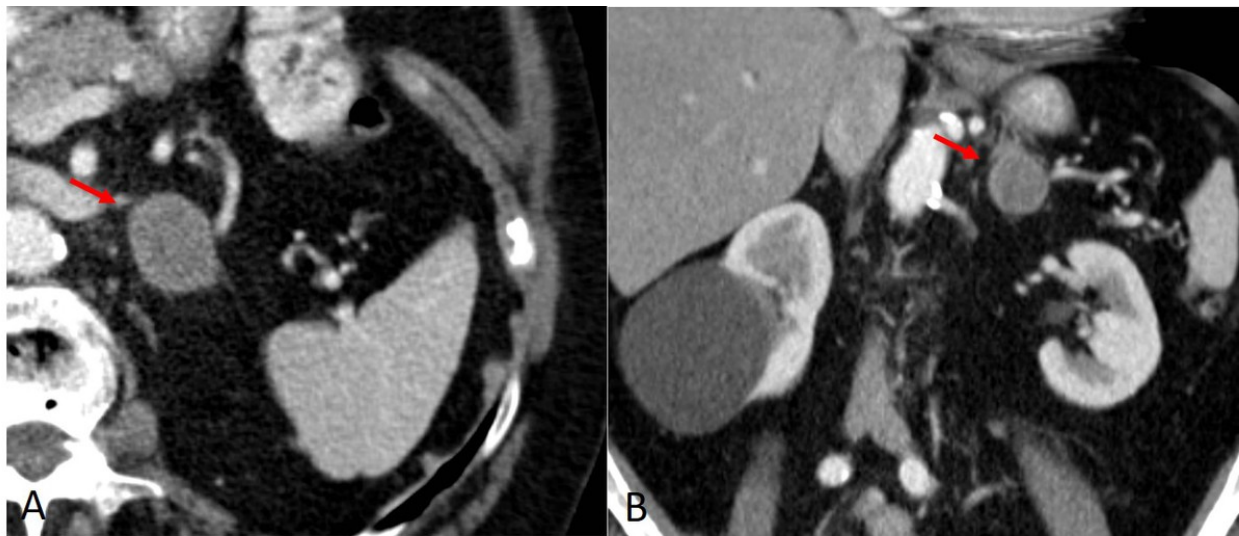


Fig. 33: Axial (A) and coronal (B) CE CT shows a metastasis in the left adrenal gland (red arrow).

© Department of Radiology, University Hospital Antwerp - Antwerp/BE



Fig. 34: Axial CE CT after administration of oral contrast shows small bowel metastasis. A shows a diffuse thickening of the jejunal wall (red arrows) and B shows multiple focal thickening of ileal bowel loops (red arrows).

© Department of Radiology, University Hospital Antwerp - Antwerp/BE

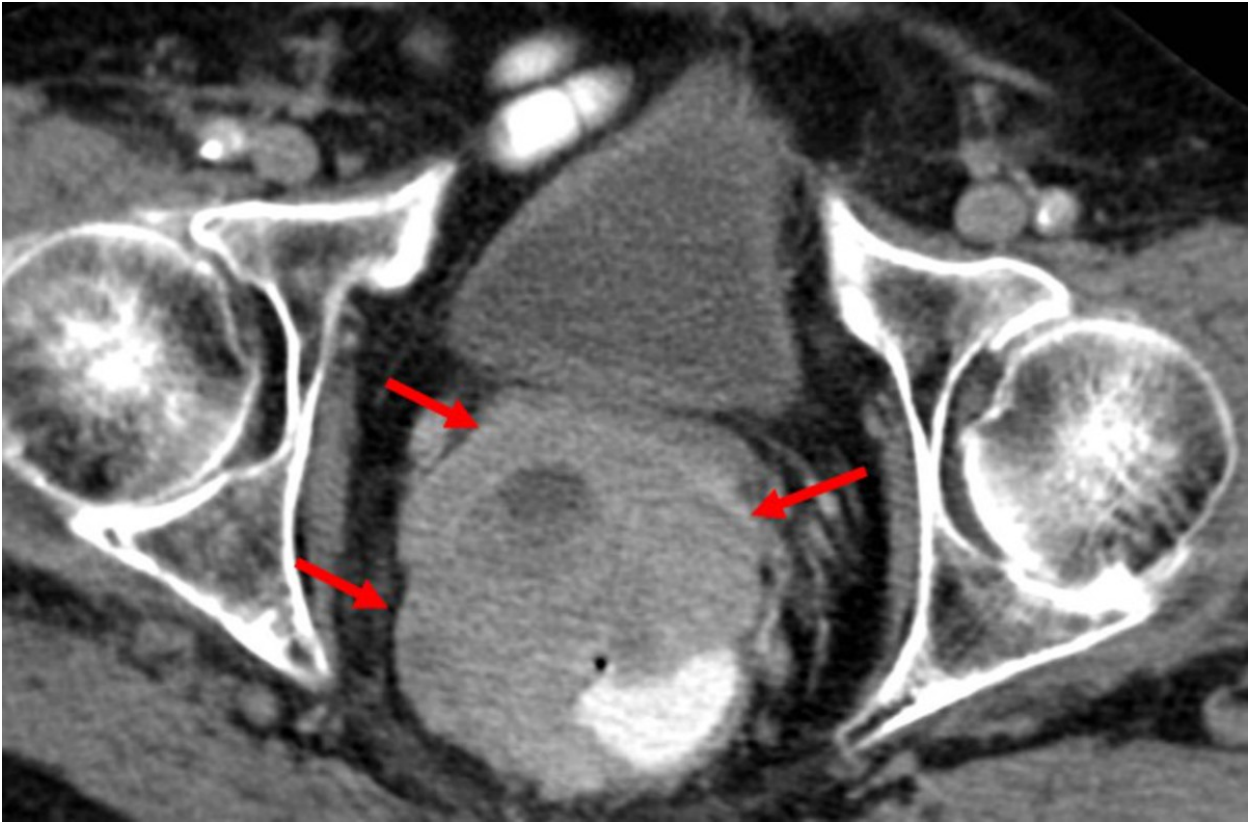


Fig. 35: Axial CE CT after administration of oral contrast shows an example of metastatic melanoma involving the rectum.

© Department of Radiology, University Hospital Antwerp - Antwerp/BE

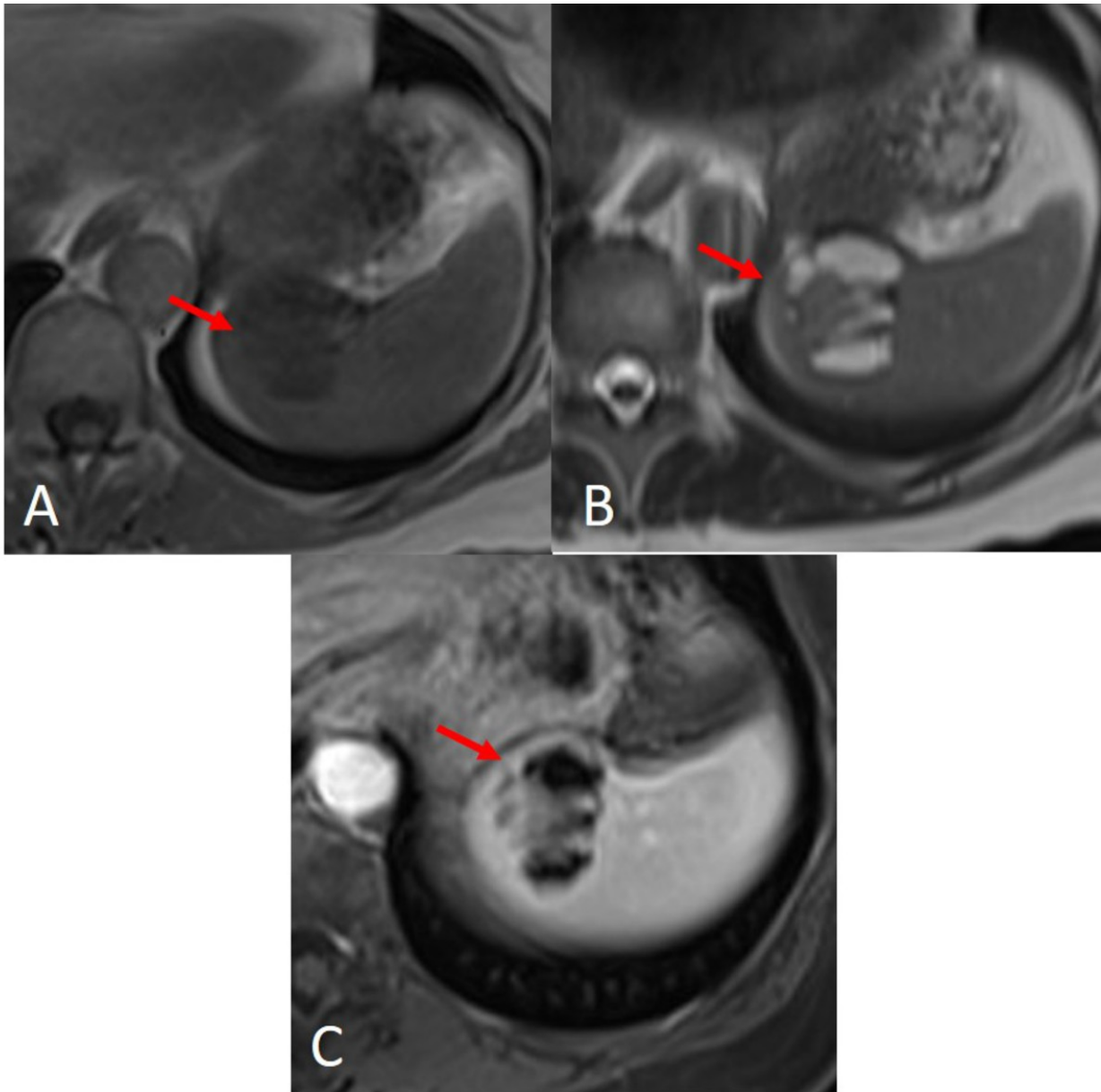


Fig. 36: T1-WI (A) shows a mass (red arrow) isointense to muscle in the spleen. On T2-WI (B) the mass has regions of iso- and hyperintensity. T1-WI after administration of gadolinium contrast (C) shows a heterogeneous enhancement of the mass.

© Department of Radiology, University Hospital Antwerp - Antwerp/BE

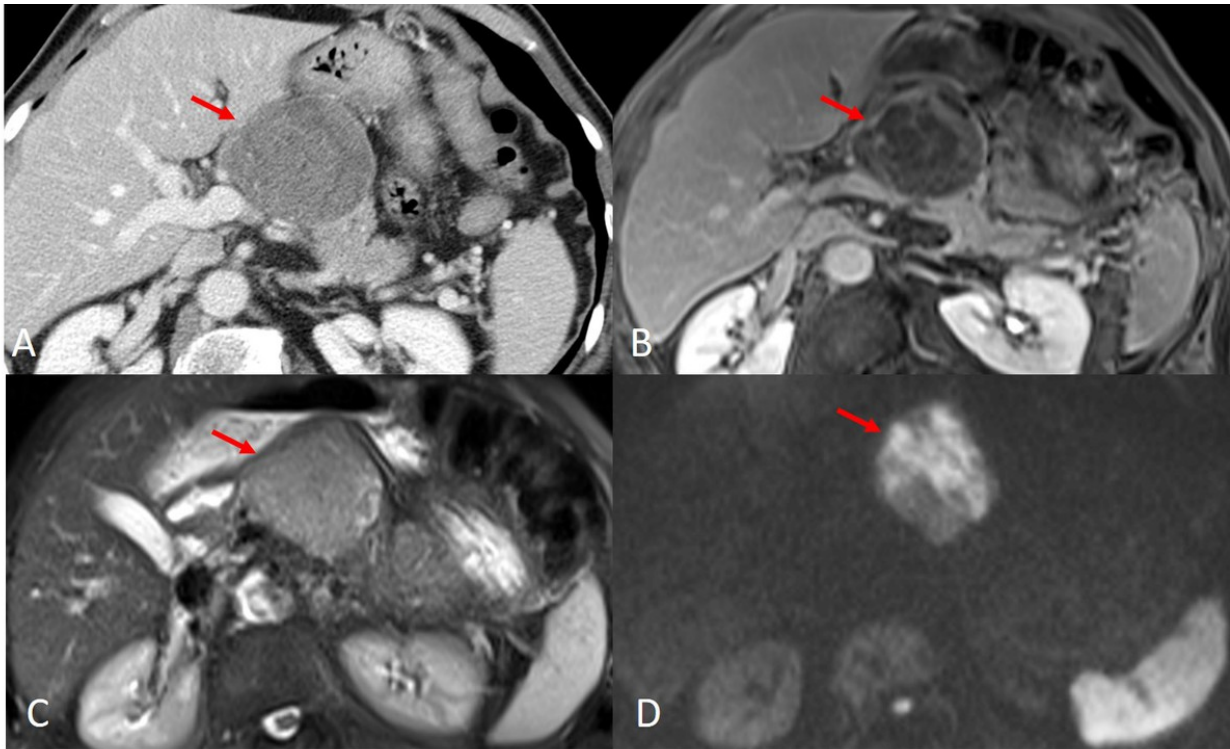


Fig. 37: Axial CT and MRI of the pancreas. CE CT (A) shows a heterogeneous enhancing mass in the pancreas. T1-WI (B) with FS shows a heterogeneous mass with regions of high and low intensity in the pancreas. The mass is hyperintense on T2-WI with FS (C). DWI (D) and ADC (not shown) shows marked diffusion restriction.

© Department of Radiology, University Hospital Antwerp - Antwerp/BE

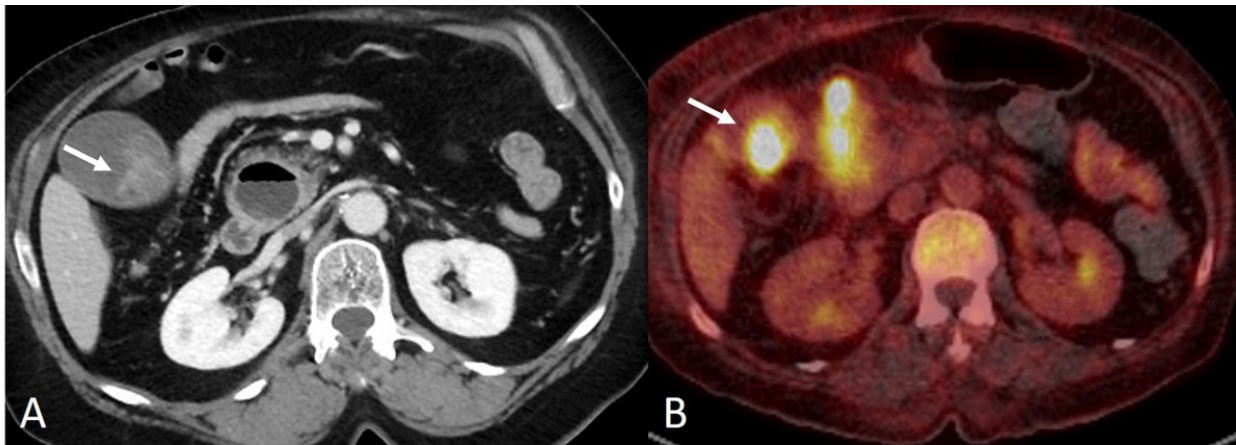


Fig. 38: Axial CE CT shows a heterogeneous enhancing mass in the gallbladder (white arrow). Fusion PET/CT shows a high metabolic activity in this lesion (white arrow). After surgical resection, histopathology showed a metastatic melanoma in the gallbladder.

© Department of Radiology, University Hospital Antwerp - Antwerp/BE

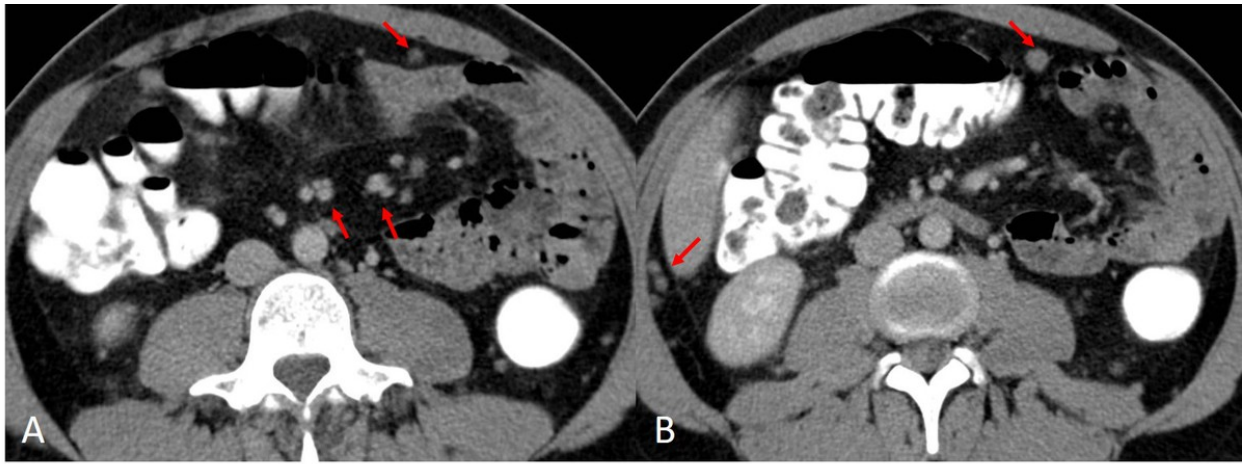


Fig. 39: Axial CE CT A and B shows multiple slightly enlarged lymph nodes located mesentery and retroperitoneal (red arrows).

© Department of Radiology, University Hospital Antwerp - Antwerp/BE

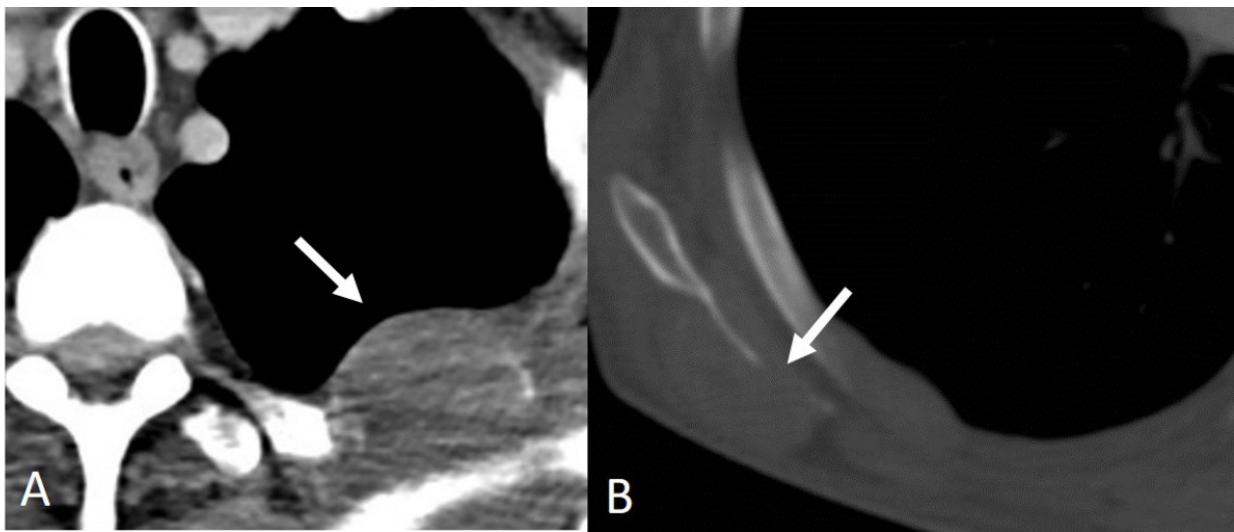


Fig. 40: CT of the chest shows an osteolytic metastasis with soft tissue component in the fourth left rib (A) and scapula (B).

© Department of Radiology, University Hospital Antwerp - Antwerp/BE

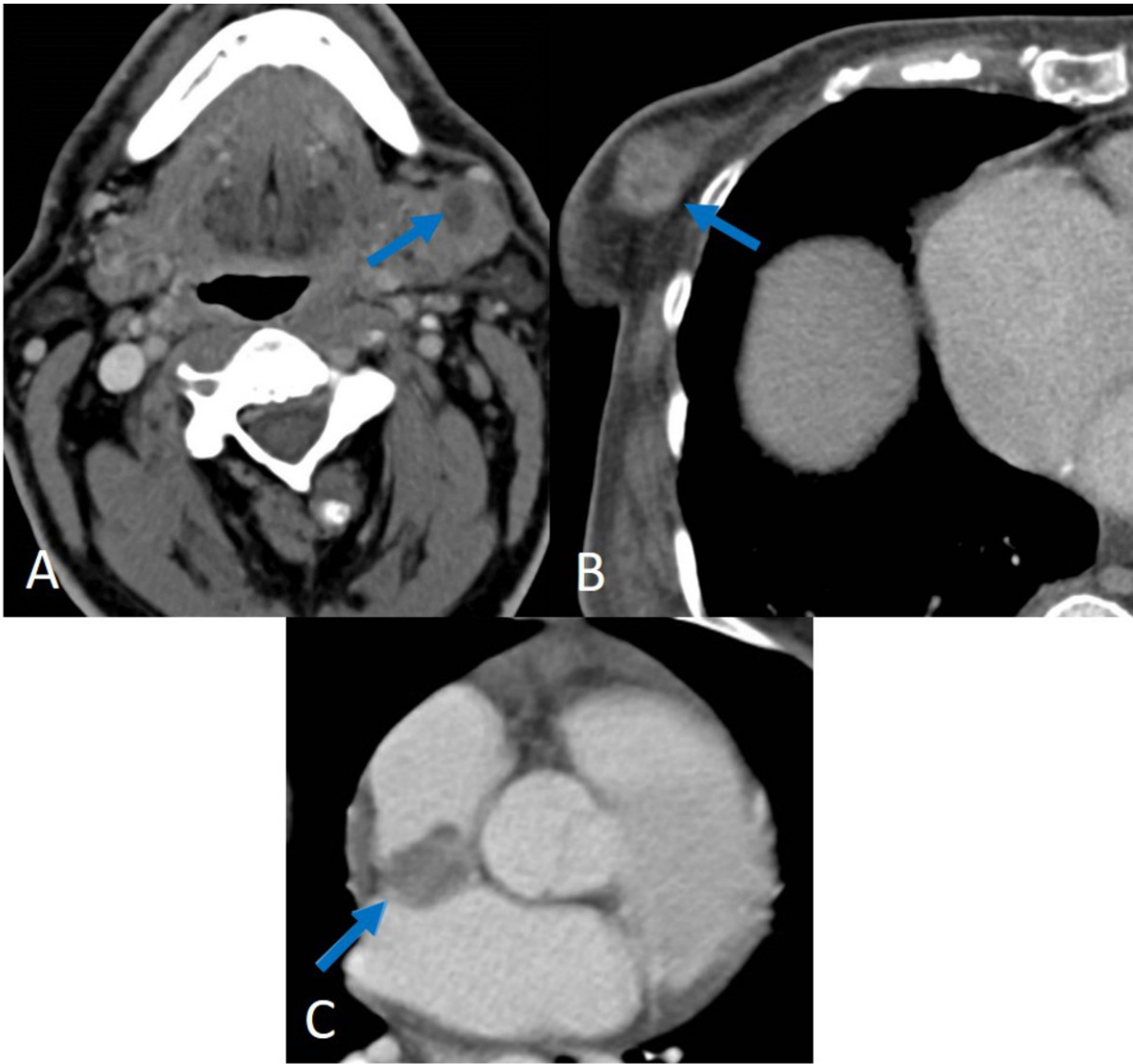


Fig. 41: CE CT shows a mass in the left submandibular gland (A), right breast (B) and heart (C).

© Department of Radiology, University Hospital Antwerp - Antwerp/BE

Conclusion

- The most frequent locations of metastasis are locoregional, lung, brain, liver or bones.
- US is used for superficial located lymphogenic spread for easily accessible areas. US is generally not used for hematogenous spread or deep locations.
- CT and PET/CT are the most used imaging modalities to evaluate hematogenous metastasis on most locations.
- MR is most sensitive and specific except for lung disease.

Personal information

Filip M. Vanhoenacker is affiliated to:

Dept of Radiology AZ Sint-Maarten, Duffel-Mechelen, University Hospital Antwerp, and University of Ghent Faculty of Medicine and Health Sciences

Address for correspondence: Rooienberg, 25, B-2570 Duffel, Belgium

References

1. Forsea A.M., del Marmol V., de Vries E., Bailey E.E., Geller A.C. Melanoma incidence and mortality in Europe: New estimates, persistent disparities. *Br. J. Dermatol.* 2012; 167: 1124-30.
2. Zbytek B, Carlson JA, Granese J, Ross J, Mihm MC, Slominski A. Current concepts of metastasis in melanoma. *Expert Rev Dermatol* 2008; 3: 569-85.
3. Voit C, Kron M, Schäfer G, et al. Ultrasound-guided fine needle aspiration cytology prior to sentinel lymph node biopsy in melanoma patients. *Ann Surg Oncol* 2006; 13: 1682-9.
4. Blake SP, Weisinger K, Atkins MB, Raptopoulos V. Liver metastases from melanoma: detection with multiphasic contrast-enhanced CT. *Radiology* 1999; 213: 92-6.
5. Balch CM, Gershenwald JE, Soong S-J, et al. Final version of 2009 AJCC melanoma staging and classification. *J Clin Oncol* 2009; 27: 6199-206.
6. Trotter SC, Sroa N, Winkelmann RR, Olencki T, Bechtel M. A Global Review of Melanoma Follow-up Guidelines. *J Clin Aesthet Dermatol.* 2013; 6: 18-26

7. Isiklar I, Leeds NE, Fuller GN, Kumar AJ. Intracranial metastatic melanoma: correlation between MR imaging characteristics and melanin content. *AJR Am J Roentgenol* 1995; 165: 1503-12.
8. Balch CM, Soong SJ, Murad TM, Smith JW, Maddox WA, Durant JR. A multifactorial analysis of melanoma. IV. Prognostic factors in 200 melanoma patients with distant metastases (stage III). *J Clin Oncol* 1983; 1: 126-34.
9. Schellinger PD, Meinck HM, Thron A. Diagnostic accuracy of MRI compared to CCT in patients with brain metastases. *J Neurooncol* 1999; 44: 275-81.
10. Patel JK, Didolkar MS, Pickren JW, Moore RH. Metastatic pattern of malignant melanoma. *Am J Surg* 1978; 135: 807-10.
11. Patnana M, Bronstein Y, Szklaruk J, et al. Multimethod imaging, staging, and spectrum of manifestations of metastatic melanoma. *Clin Radiol* 2011; 66: 224-36.
12. Peters B, Peters R, De Praeter G, Vanhoenacker F. Epidural metastatic melanoma. *Eurorad*. 2015: 12851.